Environment International 146 (2021) 106183

Contents lists available at ScienceDirect

Environment International

journal homepage: www.elsevier.com/locate/envint

Review article

Recent progress in nanomaterial-based sensing of airborne viral and bacterial pathogens

Sanjeev K. Bhardwaj [a], Neha Bhardwaj [b], Vanish Kumar [c], Deepanshu Bhatt [d], Abdelmonaim Azzouz [e], Jayeeta Bhaumik [a], Ki-Hyun Kim [f,*], Akash Deep [d,*]

[a] Department of Nanomaterials and Application Technology, Center of Innovative and Applied Bioprocessing, Sector 81 (Knowledge City), S.A.S. Nagar 140306, Punjab, India
[b] Department of Biotechnology, University Institute of Engineering and Technology (UIET), Panjab University, Chandigarh 160025, India
[c] National Agri-Food Biotechnology Institute, S.A.S. Nagar 140306, Punjab, India
[d] Central Scientific Instruments Organisation, Sector 30 C, Chandigarh 160030, India
[e] Department of Chemistry, Faculty of Science, University of Abdelmalek Essaadi, B.P. 2121, M'Hannech II, 93002 Tétouan, Morocco
[f] Department of Civil and Environmental Engineering, Hanyang University, 222 Wangsimni-Ro, Seoul 133-791, Republic of Korea

ARTICLE INFO

Handling Editor: Adrian Covaci

Keywords:
Nanomaterials
Airborne pathogens
Sensors
Infection

ABSTRACT

Airborne pathogens are small microbes that can cause a multitude of diseases (e.g., the common cold, flu, asthma, anthrax, tuberculosis, botulism, and pneumonia). As pathogens are transmitted from infected hosts via a number of routes (e.g., aerosolization, sneezing, and coughing), there is a great demand to accurately monitor their presence and behavior. Despite such need, conventional detection methods (e.g., colony counting, immunoassays, and various molecular techniques) generally suffer from a number of demerits (e.g., complex, time-consuming, and labor-intensive nature). To help overcome such limitations, nanomaterial-based biosensors have evolved as alternative candidates to realize portable, rapid, facile, and direct on-site identification of target microbes. In this review, nano-biosensors developed for the detection of airborne pathogens are listed and discussed in reference to conventional options. The prospects for the development of advanced nano-biosensors with enhanced accuracy and portability are also discussed.

1. Introduction

Air quality affects all living organisms in diverse ways. Airborne pathogenic microbes are associated with many infectious diseases such as tuberculosis, severe acute respiratory syndrome (SARS), avian flu, anthrax, and SARS-CoV-2 (Morawska and Cao, 2020; Weber and Stilianakis, 2008). In animals, airborne transmission of zoonotic pathogens, such as foot-and-mouth virus, classical swine fever, and porcine respiratory and reproductive syndrome viruses, can play a significant role in spreading infections (Chakraborty et al., 2014). In humans, major pathogens transmitted via the atmosphere include, but are not limited to, smallpox, SARS coronavirus, influenza virus, *Mycobacterium tuberculosis, Legionella* spp., *Bacillus anthracis*, and spores of many other bacteria and fungi (Siegel et al., 2007; Tang et al., 2006). The presence of dangerous chemicals, dust particulates, allergens, and infectious microbes, such as *M. tuberculosis*, *Acinetobacter baumannii, noroviruses,* and *Clostridium difficile*, in indoor air has profound health implications for humans (Cowling et al., 2013). The presence of pathogens in indoor air can affect human health both directly (via inhalation) and indirectly (by settling onto surfaces, fomites), giving rise to serious concerns in healthcare institutions, industries, and residential buildings. Possible transmission of multi-drug-resistant bacteria (e.g., *M. tuberculosis*) is another significant issue reportedly associated with persistence of pathogens in indoor air (Gandhi et al., 2010). The potential of air to serve as a vehicle for pathogen transmission has led to an upsurge in demand for effective decontamination techniques to improve indoor air quality. Meanwhile, emerging zoonotic diseases (with the ability to infect different species, as in the case of Ebola) underscore the urgent need for rapid and portable airborne pathogen sensors.

Despite the significance of timely detection of airborne pathogens, few options for rapid diagnostic tests are available to facilitate quantification of pathogens in complex matrices such as food, water, blood, and urine. In recent years, this challenging field of pathogen detection has attracted a great deal of attention from researchers. The

* Corresponding authors.
E-mail addresses: kkim61@hanyang.ac.kr (K.-H. Kim), dr.akashdeep@csio.res.in (A. Deep).

https://doi.org/10.1016/j.envint.2020.106183
Received 17 April 2020; Received in revised form 3 October 2020; Accepted 4 October 2020
Available online 25 October 2020

conventional methods of detecting airborne pathogens include cell culture-based assays, immunological methods, and polymerase chain reaction (PCR)-based molecular techniques. However, the detection of pathogens using these methods depends on post collection sample processing. Nasal swabs or blood samples are common means of sample collection for indirect air-pathogen diagnostics. These samples undergo multiple enrichment steps prior to the detection assay. In the long run, the development of direct routes of detection would be more practical to *in-situ* determine pathogen in exhaled air or blood samples without pre-enrichment.

In recent decades, biosensors have emerged as efficient platforms for the analysis of airborne pathogen samples. In addition, microfluidic bioassays have been developed for containment and rapid detection of microbes in air. Despite such progress, commercialized devices with proven performance records in real samples are yet not available. Low concentrations of microbes in air, presence of interfering factors, and inability to connect the sampling chamber with a sensing device have undermined diagnostic success. With advancements in nanotechnology, many researchers have employed the unique properties of nanomaterials (including a high surface-area-to-volume ratio) to develop efficient and sensitive detection methods. Nanomaterials have enabled miniaturization of sensing devices, leading to rapid, portable, and sensitive pathogen diagnostic systems that can detect airborne pathogens in hospitals, air vents, and airplanes and anticipate bioterrorism attacks in public spaces.

This review focuses on the use of nanosensors to detect airborne pathogens based on various principles. The first section describes common airborne pathogens and their associated diseases. The next section explores the conventional methods of monitoring pathogens in air, including the advantages and disadvantages of each method. The third section covers the merits of nanomaterials in biosensor-based detection of airborne pathogens (e.g., stability, specificity, and sensitivity). The properties and application of various nanomaterials are then compared with those of conventional methods. The review's final section discusses the challenges associated with detection of airborne pathogens in the context of future development of efficient sensors.

2. Common airborne pathogens and their associated diseases

Airborne pathogens are microbes that spread through the air via fine mist, dust, aerosols, or liquids. They are responsible for several illnesses in humans, birds, and animals. Common airborne pathogens can be classified into three broad categories: viruses, bacteria, and fungi (Fig. 1), as discussed in the following sub-sections.

2.1. Viruses

Viruses have been recognized as the major cause of many serious and fatal airborne diseases. The most common highly infectious virus, influenza, is spread through tiny droplets in the air produced by coughing, talking, and sneezing (FluView, 2011). Data from the Centers for Disease Control and Prevention estimated that, in 2017–18, more than 48.8 million illnesses, approximately 959,000 hospitalizations, and 79,400 deaths were associated with influenza in the U.S. alone (D'Amore et al., 2019). The H1N1 strain (influenza A) is one of the deadliest known influenza strains and was responsible for nearly 60 million infected cases in US alone during 2009 pandemic (FluView, 2011; Novel, 2010). Its short incubation time of approximately 2–3 days, delayed onset of symptoms (after approximately 12 h of infection), and genetic mutations create challenges in the effort to control and treat influenza A strains (Cao et al., 2011; Fiore et al., 2008; Nobusawa and Sato, 2006).

Another highly infectious viral disease, avian influenza, has various subtypes, including H5N1, H5N2, H3N2, and H7N9. The virus primarily affects poultry and livestock but can be transmitted to humans and has imposed heavy burdens on national economies worldwide (Chantong and Kaneene, 2011; Coker et al., 2011; Jonduo et al., 2013). In addition, the virus mutates quickly to develop panzootic strains that are major causes of concern among healthcare agencies. Also, there is a growing potential threat in the form of bioterror attacks that deploy engineered strains of the highly pathogenic H5N1 virus (Kotwal, 2008; Morens et al., 2012).

The rubella virus also poses serious health threats. It is transmitted through droplet secretions generated by sneezing or coughing. This virus has a typical growth incubation period of 2 weeks (Fronczek and Yoon, 2015). Rubella is responsible for German measles, which mainly affects

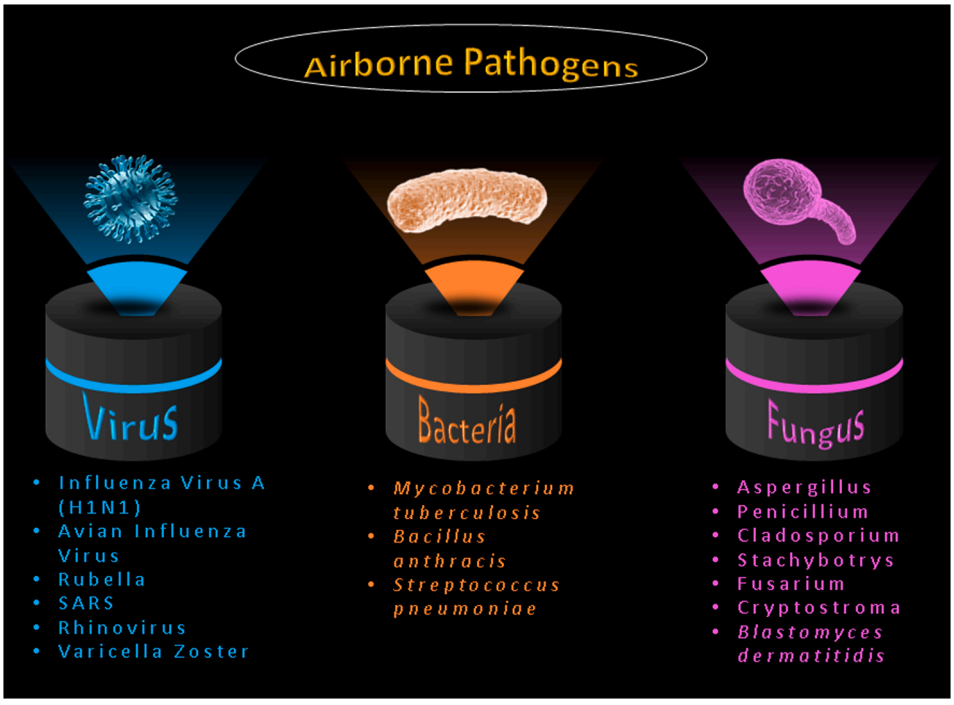

Fig. 1. Classification of common airborne pathogens.

developing nations (Organization, 2013; Reef et al., 2011; Rota et al., 2011). Most cases of rubella infection can be treated with mild medications, but serious complications such as blindness can also occur. Congenital rubella syndrome causes miscarriages during pregnancy in approximately 20% of patients (Atreya et al., 2004; De Santis et al., 2006).

In addition, SARS (Severe acute respiratory syndrome) has been associated with a lethal virus responsible for causing acute respiratory distress and even death. A member of the coronavirus family of viruses, it was first identified in 2003 during an epidemic in China. SARS was reported in more than two dozen countries that year and was responsible for more than 8000 cases, including 774 deaths (Anderson et al., 2004). The major symptoms of SARS, which include coughing, high fever, chills and shakes, and difficulty breathing, generally appear after 2–10 days of contact with the virus. Supportive treatments are available, including antibiotics, ventilators, and antiviral drugs. Research is underway on vaccine development. Other common airborne disease-causing viruses include rhinovirus (common cold), varicella-zoster virus (chickenpox), and rubeola virus (measles) (Cooper, 2012). The diseases caused by these viruses are widespread, and vaccination campaigns have been mounted by nations worldwide to control their spread. For instance, the COVID-19/SARS-CoV-2 (2019 pandemic) has posed a great global threat with a significant economic loss. Emergency response measures including travel bans and lockdowns (to restrict the movement of people inside the specific zones) have been imposed by the globally in many countries to contain the spread of the virus (Tian et al., 2020). Worldwide efforts have been directed towards development of vaccines in order to combat the contagious virus.

2.2. Bacteria

Bacteria belong to a community of microbes that humans encounter with high frequency. These microorganisms are often responsible for frequent outbreaks of airborne disease through microbial contamination. *Mycobacterium tuberculosis*, *Bacillus anthracis*, and *Streptococcus pneumoniae* are responsible for several airborne diseases (Grisoli et al., 2009; Källenius et al., 2008). *M. tuberculosis* is responsible for tuberculosis, one of the more widely spread diseases and is highly contagious. It is a Gram-positive bacteria responsible for causing tuberculosis (TB) and other complications, such as meningitis and pneumonia (Fronczek and Yoon, 2015). The bacteria normally possess a doubling time of 4–24 h (in-vitro), with an incubation period of 4–6 weeks (Fronczek and Yoon, 2015; Gill et al., 2009). TB is a highly communicable disease with a low infectious dose (ID_{50}) of <10 colony-forming units (CFU) and can spread through air via sputum or saliva droplets generated by coughing (Lin et al., 2012; Millet et al., 2013). The disease is now the most common global bacterial disease, infecting some 14 million persons every year and causing nearly 2 million deaths (WHO and WH, 2012). Although great efforts have been made to control TB, antibiotic-resistance has led to its reoccurrence (Russell et al., 2010).

B. anthracis is a Gram-positive bacterium that can cause serious and lethal infections (Spencer, 2003). It causes anthrax in humans but is not contagious. However, it is an endospore-forming bacterium that can survive under harsh environmental conditions and for extended periods in its dormant state (Kuris et al., 2014). The high stability and low ID_{50} (Median Infectious Dose, i.e., the infective dose of microorganisms that will cause 50% of exposed individuals to become ill) of 10,000 spores make it a notorious organism on a global scale. Mortality rates approaching 90% due to anthrax have been recorded in past; even with antibiotic treatment, mortality can be as high as 45% (Leffel et al., 2012; Sweeney et al., 2011). The spores of *B. anthracis* are also used as biowarfare agents due to their high lethality and low infectious dose, making it a national security concern.

S. pneumoniae is a Gram-positive, facultative, aerobic bacterium that can be spread through coughing, sneezing, and close contact with infected hosts. It can cause many airborne diseases, including pneumonia, adult meningitis, ear and sinus infections, and septicemia in immune-deficient patients (Fronczek and Yoon, 2015). The bacteria generally infect immune-compromised individuals, older adults (more than 65 years), and children (<2 years) (Lee et al., 2010; Magnus et al., 2011). An estimated 60% of the world's bacterial infections are caused by 10 common serotypes of *S. pneumonia* (Donkor et al., 2013; Johnson et al., 2010). Such infections are highly transmittable, as the bacteria has a short incubation period (1–3 days), low doubling time (30 min), and an ID_{50} hypothesized to be as low as 10^4 to 10^8 CFU (Lynch III and Zhanel, 2010). An annual global death toll of approximately 1.2 million infants has been ascribed to pneumonia, which points to its significant pathogenic threat (O'Brien et al., 2009). Efforts must be made toward its control in hospitals and other susceptible environments to reduce the morbidity, mortality, and national economic burden caused by this organism.

2.3. Fungi

The presence of fungi in both indoor and outdoor environments is a potential threat to human health. Several fungal species are present in our homes in food and other materials, including damp paper, textiles, and wood. Fungal species produce spores, allergens, toxins, and volatile organic compounds that can cause respiratory illnesses such as asthma, inflammation in nose and sinuses, and hypersensitivity pneumonitis. There is, therefore, a need to monitor the composition and concentration of airborne fungi and their spores to manage their potential threats.

Various indoor airborne fungi have been reported in the literature, including *Aspergillus, Penicillium, Cladosporium, Mucor, Stachybotrys, Absidia, Alternaria, Fusarium*, and *Cryptostroma*. Among them, major health risks are often reported to be posed by *Candida, Aspergillus, Histoplasma,* and *Penicillium*. In hospitals, most fungal infections are caused by *Candida* and *Aspergillus* as they occur naturally in exterior environments and enter as spores or active fungi attached to dust particles (Augustowska and Dutkiewicz, 2006; Rainer et al., 2001). Aspergillus is a common mold that causes aspergillosis in humans with weakened immune systems or lung diseases. It causes mainly allergic reactions and infections in lungs and other organs.

Among other fungi, *Blastomyces dermatitidis* is a highly pathogenic dimorphic fungus present in moist soil and decomposed matter (Baumgardner and Paretsky, 1999). Inhalation of its spores can infect lungs and spread to other body parts. The fungus grows in the form of yeast and can spread like cancer cells through the blood, leading to severe infection, which may be fatal if not diagnosed and treated promptly. The symptoms of illness caused by this fungus are similar to those of influenza or pneumonia and thus are often misdiagnosed by physicians, resulting in inappropriate treatment. New methods are therefore needed to provide reliable, accurate, and fast detection results.

3. Conventional methods for detection of airborne pathogens and their limitations

The determination of airborne pathogens generally consists of a two-step procedure. The first step includes the collection and enrichment of pathogens. Sample enrichment/concentration is a key pre-requisite for ultimate detection owing to very low numbers of virus/bacteria/fungi particles within the air. The pathogen enrichment step not only improves the sensing efficiency of any sensor but also is helpful in reducing the sensing time (Jing et al., 2013). The details of the sampling and detection techniques are discussed in the following sub-sections.

3.1. Conventional and nanomaterials-based detection techniques

Efficient samplers can greatly improve the performance of sensors. A number of strategies have been explored to connect sample collection units with analyte monitoring units to develop numerous types of sampling, e.g., impaction, impinging, and filtering (West and Kimber,

2015). In case of impaction (deposition), adhesive-coated surfaces are typically used to efficiently collect airborne particles. Petroleum jelly (Vaseline) is one of the most explored materials in passive impaction. The passive impaction of airborne particles takes place onto petroleum-jelly coated microscope slides or thin glass rods. Although the method is relatively cheaper but is linked with problem of quantification of spores and particles. The microtiter immunospore (MTIS) trapping device is an advanced version of impaction sample collectors (Kennedy et al., 2000; Wakeham et al., 2004; West and Kimber, 2015). This collector is portable, making it useful for direct applications, similar to that used in ELISA (Kennedy et al., 2000). The MTIS is composed of a suction system and microtiter wells. A multi-well system (32 wells) is beneficial in analyzing multiple analytes in a single sample. The MTIS has been tested as a sample collector and for determination of spores of airborne pathogens such as *Brassica oleracea* (Kennedy et al., 2000), *Mycosphaerella brassicicola* and *B. cinerea* (Kennedy et al., 2000; Wakeham et al., 2004), *Cladosporium cladosporioides* (Wakeham et al., 2004), and *Lycopodium clavatum*, *Penicillium roqueforti*, and *Erysiphe cruciferarum* using ELISA. The critical shortcomings associated with the MTIS have restricted its application as a modern point-of-care sensing system. These shortcomings include slow sampling, requirement for separate culture enrichment procedures, and need for an entirely separate detection component (i.e., ELISA) (Fronczek and Yoon, 2015).

In impingers, collection of air samples proceeds with bubbling through a liquid, which is an efficient method of capturing small particles (West and Kimber, 2015). However, this method is also associated with some limitations, i.e., small volume sampling, unavailability of universal liquid, and loss of liquid due to evaporation (if used for long periods) (West and Kimber, 2015). On the basis of miscibility of sample particles, a specific liquid is required to capture sample particles. For example, to capture hydrophobic spores, ethanol or a surfactant diluted with water is suitable. Many other commonly used air sample collectors also face shortcomings. Slow flow rates and blockings are common if filters are used as a sampling medium (West and Kimber, 2015). Moreover, in a majority of sample collectors, separating airborne particles from the sample collector requires additional steps for sensing of an analyte. A portable sampler is required to directly pass the analyte to the sensor surface.

Sample collection methods for microfluidic immunosensing reportedly suffer from similar lengthy operational procedures (Kwon et al., 2014). Viruses first are collected in a filter inside the sampler. The collected viruses are then forced through the filter by a syringe after being dissolved in liquid. Because of this pre-treatment step, the sensor cannot perform real-time analysis. Likewise, a microfluidic system was tested for determination of *M. tuberculosis* (Jing et al., 2014). An additional enrichment step was used for efficient sensing of *M. tuberculosis*. This bacterial immunoassay can be performed in 50 min (20 min for enrichment and 30 min for analysis) with a detection limit of 100 CFU/mL. The main problem associated with this method is the requirement for additional enrichment and cell lysis steps, which again lengthen the process. The introduction of nanomaterial-based approaches has improved the performance of such sensors. The application of nanomaterials intended for sensing of airborne pathogens is discussed in Section 4.

Hospodsky et al. (2010) reported the use of filters to capture bacteria from aerosol samples for quantitative determination of *E. coli* and *Bacillus atrophaeus* based on qPCR methods (Hospodsky et al., 2010). The developed method involved multi-step capturing procedures to maximize the number of particles collected by the filters. It was postulated that recovery of DNA from filters was 10 to 24 times lower than the actual level of DNA in the aerosol. A porous medium was used as a sampler in another study to capture bacterial species (*Pseudomonas* and *Bacillus*) from the air for PCR-based quantitation (Agranovski, 2007). In another study, Teflon filters were used to detect rhinoviruses using RT-PCR in aerosols (Myatt et al., 2003). Sensing of these viruses was entirely dependent on collection efficiency of the sampler (Teflon filters). The sampler was also subjected to other shortcomings, such as pretreatment of collected sample (e.g., sample extraction).

An improved sampler was employed to capture three aerosolized viruses, i.e., rhinovirus, influenza A, and parainfluenza (Huynh et al., 2008). The captured viruses were extracted and tested with RT-PCR. These authors found that the employed method was unfeasible for rapid point-of-care applications due to laborious procedures, including sample extraction for PCR-based assay. Likewise, only modifications in the sampler were observed in PCR-based virus sensors (Agranovski et al., 2006; Lednicky and Loeb, 2013; Pyankov et al., 2007). However, common problems associated with treatment procedures in PCR remain unresolved.

The use of sampler is also crucial for the effective sensing of viruses using nanomaterials. An efficient sampler can increase the utility of nanomaterials-based sensors for viruses. A number of studies focused on the sampling of virus particles to show the importance of sampler in the development of virus sensors (e.g., SARS-Cov 2 sensor) (Rahmani et al., 2020). The selection of sampler is majorly dependent on the type of target virus. For example, the H1N1 viruses can be collected from the exhaled air (specifically aerosols generated during coughing) of the infected patient for microfluidic based sensing (Kwon et al., 2014). In contrast, the collection of H1N1 from normal air is very difficult due to lower level of viruses.

In a study, the button aerosol sampler was used to collect H1N1 viruses from mock classroom (Kwon et al., 2014). The aerosol particles generated by mock human (using nebulizer) was injected for 3 s using pressurized nitrogen with velocity of 11 m/s. After 3 min of ventilation, the button aerosol sampler was used to collect aerosol samples for 30 s. Three different locations were used to collect samples. It is worthy mentioning that the sampler is fitted with a filter (1820-070; Whatman) and the captured virus particles on filter were dissolved by soaking the filter in PBS (150 μL). The dissolved virus particles were then removed with by syringe for further processing (Kwon et al., 2014). Likewise, corona/lens-based collection procedure has been used effectively for the capturing of airborne analytes (Fang et al., 2014). The basis mechanism of corona/lens-based collector is the charging of analyte particle using corona and collection of the analyte particles on the oppositely charged collecting surface.

Likewise, the impaction on a gel approach was used to collect viruses for their optical detection (Ferreira et al., 1999). This sampler mainly consisted of vacuum pump (flow rate of 1001 min^{-1}), perforated plates, and agar containing Petri plates. This sampler was arranged in a way that the air containing particles < 10 μm were directly diverted to the agar containing Petri plates. For the sensing of SiNW-based sensing of H1N1 virus, exhaled breath condensate (EBC) collection device was used as a sampler to collect virus particles (Shen et al., 2012). In general, ECB was composed of four parts, (1) and (2) collection device cover and base, (3) ice layer, and (4) −70 °C treated hydrophobic layer. A hole in the device cover was used for the inlet of exhaled breath, while the ice layer was used to cool the hydrophobic layer. The low temperature of the hydrophobic layer (parafilm) led to immediate condensation of the inlet air in the form of small droplets. The condensed droplets were then recovered using DI water to detect the presence of viruses.

The pathogen enrichment process is also crucial for the efficient detection of pathogens. The enrichment of pathogens in air samples can be performed in multiple ways, e.g., sedimentation. microfluidic chip, and suspension solution-based methods (Jing et al., 2013; Liu et al., 2018). For these methods, culture dishes (e.g., Lysogeny broth; LB culture dish), chip microchannels, and buffer can be employed, respectively. In case of microfluidic channels, the laminar flow of fluid can be damaged by modifying the channel structures (e.g., by introducing staggered herringbone structure) for the efficient capturing of pathogens. As such, other methods such as wet-cyclone and gravity-driven cell enrichment were also found efficient to enrich the pathogens in air samples (Cho et al., 2019a, 2019b).

3.2. Detection methods

A variety of methods has been used to detect different airborne pathogens (Fig. 2), ranging from simple colony-counting methods to immunological, PCR-based, and spectroscopy techniques as discussed in the following sub-sections.

3.2.1. Cell culture and colony-counting techniques

Cell culture and colony-counting techniques are the simplest methods of isolating, culturing, and quantifying cells. These techniques generally involve collection of cells on a selective or differential medium that allows the proliferation of the microorganism of interest. For airborne pathogen detection, the principle is the same: collected air samples are cultured on a solid medium and enriched for colony-counting and further analysis using culture method. Although efficient, the method suffers from a lack of a comprehensive point-of-care system and a requirement for manual labor. Such analyses become difficult when the sample quantities are large. For instance, Hsiao et al. used CHROMagar media, filters, and chambers to detect antibiotic-resistant *Enterococcus* species (Hsiao et al., 2014). However, lack of automation and long assay times were limiting factors. Relative humidity also plays a role in culture efficiency, as shown by Rule et al., where the efficiency of different aerosol collection systems was compared (Rule et al., 2009). They showed that a minimum of 15% relative humidity is required. The entire detection process took 16 h, which is undesirably long.

3.2.2. Immunological detection methods

Immunological methods are widely used for the detection of airborne pathogens. Apart from their simple detection platforms and good detection performance, these methods cannot be implemented without a bio-recognition element (e.g., ELISA, radioimmunoassay, and microfluidics) and pose sampling-related challenges. Variants of immunological detection methods and different samplers involved in these methods are discussed in subsequent subsections. Immunological methods such as enzyme-linked immunosorbent assay (ELISA) and radio-allergosorbent test (RAST) are the most common of the conventional methods (Burge and Solomon, 1987; Kwon et al., 2014; Mairhofer et al., 2009; Skládal et al., 2012). These methods are well known for their analytical speed, sensitivity, and specificity. Despite their ability to accurately determine analyte concentration, these techniques also suffer from unavoidable drawbacks. With ELISA, multiple and tedious pipetting and rinsing are required (Fronczek and Yoon, 2015), while RAST involves mandatory use of a radioactive tag (e.g., ^{125}I) that restricts its applicability (Burge and Solomon, 1987). Moreover, a separate and special assembly process is required for collection and monitoring of airborne pathogens. The reduction in the complexicity of the procedures, direct sensing of analyte pathogens, portable sensing machinery, safe/easy availability of radioactive tag, and on the spot signal general could govern the real time analysis of pathogens using these techniques.

3.2.3. PCR and nucleic acid–based detection

PCR or nucleic acid–based techniques for detection of airborne bacteria and viruses are also capable of producing sensitive and selective signals. In many cases, such techniques are relatively efficient in determining the pathogen level in bioaerosol samples. Progressive changes have helped overcome the infamous drawbacks of PCR (e.g., need for laborious steps that can take up to 4 h) (Fronczek and Yoon, 2015). Use of conventional PCR is also restricted by many limitations (e.g., involvement of complex treatment steps, such as nucleic acid extraction/purification and thermocycling, and requirement for separate imaging tool such as gel electrophoresis). Although PCR can be employed to detect viruses comprising DNA in their genome, it cannot be used for viruses containing RNA as their genetic material. In such cases, reverse transcription PCR (RT-PCR) is employed. Use of an additional cDNA template synthesis step makes this process even more complicated and time-consuming.

Advancements in PCR have introduced processing kits (e.g., primer kits and nucleic acid extraction kits), real-time quantification, and portable instrumentations. However, for detection of airborne bacteria and viruses, PCR-based approaches remain time consuming. In many cases, PCR-based methods have been employed to determine the presence of bacteria and viruses in air samples (Agranovski, 2007; Alvarez et al., 1994; Hospodsky et al., 2010; Sawyer et al., 1994; Stetzenbach et al., 2004). However, these method involves a number of processing steps, including collection of samples, sample preparation, and PCR.

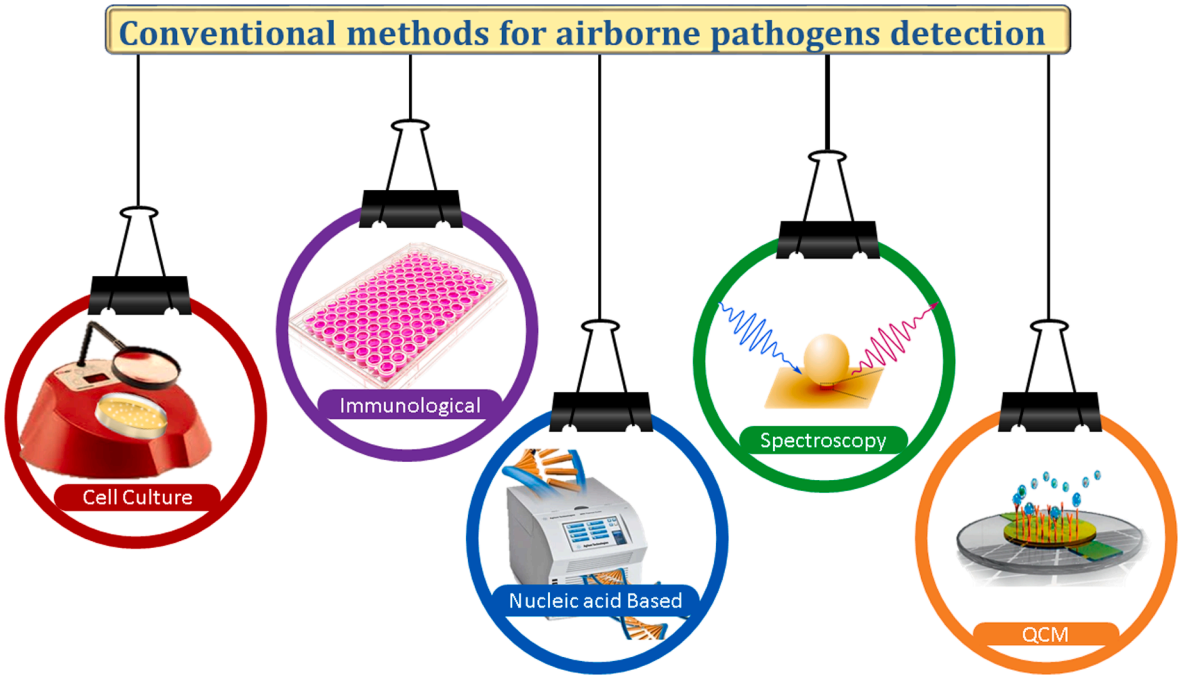

Fig. 2. Conventional techniques for recognition of airborne pathogens.

Once all are put together, these steps take more than 2 h to limit its application to real-time monitoring. However, incorporation of semi-automation and microfluidics in PCR-based technologies has been an option to reduce the total analysis time (e.g., up to 70 min) (Inami et al., 2009; Jiang et al., 2014).

Till now, PCR-based approaches have also been employed to detect various airborne viruses, e.g., influenza (Huynh et al., 2008; Pyankov et al., 2007), vaccinia (Agranovski et al., 2006), porcine circovirus (Verreault et al., 2010), rhinovirus (Huynh et al., 2008; Myatt et al., 2003), parainfluenza (Huynh et al., 2008), H3N2 viruses (Lednicky and Loeb 2013), rhinoviruses (Myatt et al., 2003). Nonetheless, the requirement of separate sample collection and detection assembly, multiple step procedure, and manual operation restricted the use of these PCR-based detection methods as real-time sensing device. The automation, reduction in number of steps, direct sensing of target pathogens, and sensor portability could be beneficial in enhancing the possibilities of these sensors for real time analysis.

To summarize, PCR or nucleic acid–based methods require further advances in automation and real-time monitoring of bacteria and viruses. Introduction of a new sampling system that can directly and automatically deliver signals or capture pathogens to a detector may help address the shortcomings associated with present PCR-based detection methods.

3.2.4. Other techniques

In addition to the conventional techniques, a few other approaches (e.g., acoustic and optical measurement-based) have been employed to detect airborne bacteria and viruses. In a typical example of a quartz crystal microbalance (QCM)-based sensor, the vaccinia virus was detected at a detection limit of 10 particles/mL (Lee et al., 2008). Known levels of virus suspension (8.5×10^8 to 8.5×10^{10} particles/mL) were prepared and exposed to the QCM crystal surface. Upon exposure, the QCM crystal captured viruses with a shift in resonance frequency proportional to the concentration of particles. In another report on QCM-based sensors, nebulized influenza virions were detected with a gold-modified QCM crystal–based immunochip (Owen et al., 2007). The immunochip exhibited a detection limit of 4 virus particles/mL. As with the QCM sensor, the performance of the immunochip sensor was not replicated in real samples. As no sampler was used in either of the above QCM-based studies, it is not clear whether the methodology will work for real breath or air samples. Such systems are also subject to a number of shortcomings, such as bulky instrumentation, unsuitability for point-of-care analysis, expense, requirement for large amounts of samples, and signal instability (Fronczek and Yoon 2015).

The ability of an aerosol fluorescence sensor to determine bacterial (e.g., *E. coli* and *B. subtilis*) levels in aerosols (Jung et al., 2012) has also been explored. This sensor uses the fluorescence properties of amino acids present in living organisms. As sensing of an analyte depends upon fluorescence of amino acids, the sensor can discriminate biological from non-biological materials but cannot be employed to differentiate viruses or bacteria. In addition, need for expensive and bulkier instrumentation also limits its applicability toward the point-of-care diagnosis. The same problem can be observed with sensors on similar instruments (Kang et al., 2014; Pinnick et al., 1998; Wilson and DeFreez 2004). Other techniques, including surface plasmon resonance (SPR) (Marusov et al., 2012; Usachev et al., 2014), Raman spectroscopy (Sengupta et al., 2007; Sengupta et al., 2005), mass spectroscopy (Angelakis et al., 2014; Tobias et al., 2005), and flow cytometry (Orsini et al., 2008), have also been explored. These sensing techniques displayed acceptable sensitivity and analytical speed. Nonetheless, they suffered from shortcomings including high cost, bulky instrumentation, complex operational steps, off-line sampler assembly, non-specificity, and inability to monitor pathogens in real time.

Overall, the utility of conventional sensors and detection techniques is limited with respect to point-of-care and real-time analyses. To fabricate a real-time and point-of-care-specific sensor for bacteria and viruses, a sensor should include an online sampler, rapid and sensitive analysis system, fully automated operation, minimum processing steps, and specificity components. Nanomaterials can help improve the efficiency and quality of aerosol sensors, and their use is expected to offer many benefits, especially in reduction of analysis time. Details of the applicability of nanomaterial-based sensors are discussed in the next section.

4. Nanomaterial-based detection of airborne pathogens

Nanomaterials are well-established matrices for development of biosensors. Multiple nanomaterials with transduction functionings have been exploited to develop optical, electrochemical, and piezoelectric bio- and chemo-sensors. The potential utility of various nanomaterials (such as carbon nanotubes (CNTs), graphene, gold nanoparticles, silver nanoparticles, and quantum dots) has been explored to develop detection platforms that recognize a variety of airborne pathogens. Optical and electrochemical biosensors (Fig. 3) have gained popularity because of their operational simplicity, suitability for point-of-care, and field applications due to their small size. For the detailed discussion, this section has been divided into optical and electrochemical sensors.

4.1. Optical sensing of airborne pathogens

Optical biosensors can sensitively detect optical signals generated in response to binding of analytes with probes. Various optical biosensors have been reported based on several detection modes, including colorimetric, fluorescence, plasmonic-band, and energy transfer. Of these, colorimetry is the most popular owing to its simplicity and convenience of use. In a colorimetric biosensor, a signal is generated in the form of a color that can be easily interpreted by an untrained naked eye, and there is no requirement for bulky (or complex) instrumentation or tedious intermediate steps. For example, a colorimetric technique has been developed and exploited for detection of H3N2 virus using the peroxidase activity of specific antibody conjugated gold carbon nanotubes (Ab/Au-CNTs) (Ahmed et al., 2016). The target viruses were initially bound to the wells of a 96-well flat bottom microtite plate and then allowed to interact with specific antibodies conjugated with Au-CNT nanohybrids. The unbound Ab/Au-CNT nanohybrids were washed out from the wells and the immunocomplex formed was detected using peroxidase activity of Au-CNTs. The detection mechanism was based on oxidation of the chromogenic substrate 3, 3′, 5, 5′-tetramethyl-benzidine (TMB) in the presence of H_2O_2 to yield a unique blue color (Fig. 4). The amount of color developed was proportional to analyte (H3N2) concentration in the medium. The assay yielded rapid results (in less than 10 min) while offering approximately 500 times the sensitivity of commercially available immunochromatography kits (Ahmed et al., 2016). In a similar study, the peroxidase activity of graphene-gold nanoparticles was tested for colorimetric detection of norovirus-like particles (Ahmed et al., 2017). The developed biosensor displayed a linear detection range of 100 pg/mL to 10 μg/mL, with a detection limit of 92.7 pg/mL (approximately 112 times more sensitive than ELISA methods). The method was pronounced to be 41 times better than available commercial diagnostic kits.

In some cases, peroxidase activity of nanomaterials requires stimulation as the catalytic activity of nanoparticles is reduced upon surface conjugation with biomolecules. For instance, mercury ions (Hg^{2+}) were employed as a stimulant for detection of respiratory syncytial virus (RSV) using the peroxidase activity of gold nanoparticle–graphene oxide (AuNP-GO) hybrids (Zhan et al., 2014). The peroxidase activity of Ab conjugated AuNP-GO (Ab1/AuNP-GO) was efficiently improved in the presence of Hg^{2+} due to metallophilic interaction between Hg^{2+}-Au. The secondary antibody (Ab2) bound microtiter wells were also used for the detection of RSV based on a sandwich immunoassay format. The immunocomplex formed (Ab2/RSV/Ab1/Hg^{2+}-AuNP-GO) in the presence of target analyte (RSV) was detected by catalysis of TMB in the

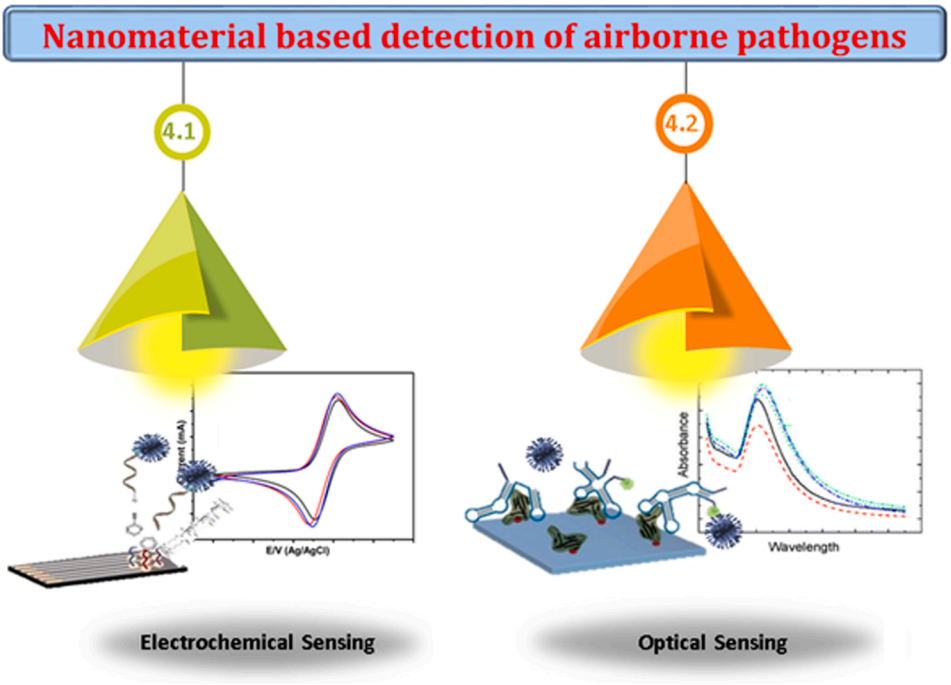

Fig. 3. Schematic of electrochemical and optical sensing of airborne pathogens using nanomaterials.

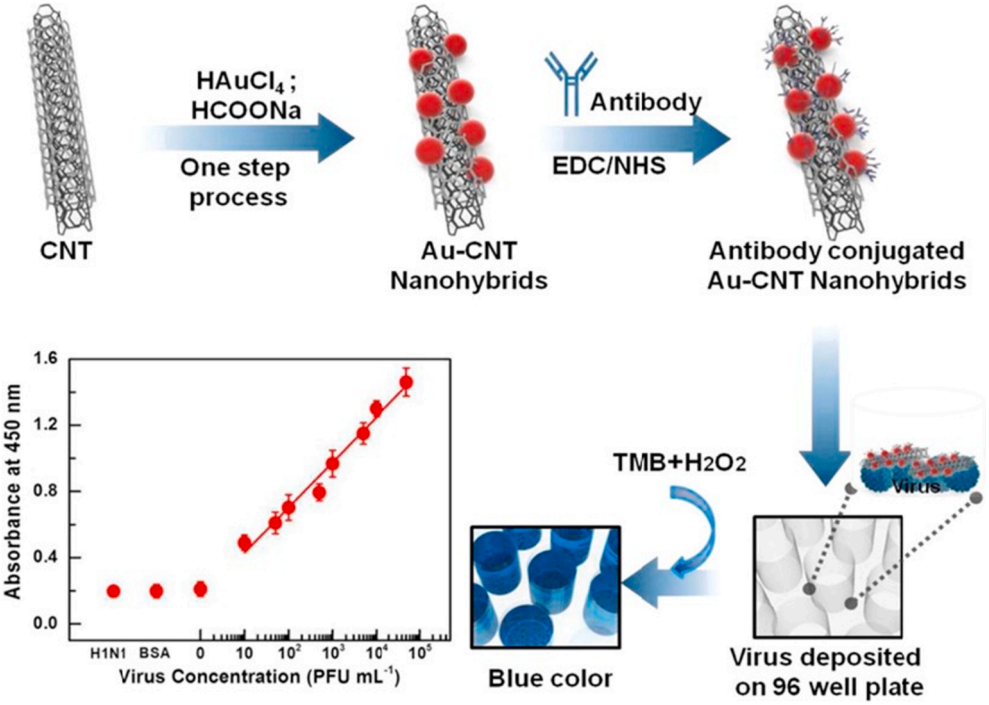

Fig. 4. Detection of H3N2 using peroxidase activity of Au-CNTs (Ahmed et al., 2016).

presence of H_2O_2. The assay time was reported to be approximately 20 min. Another approach used for visual detection of flu viruses depends on complexation (aggregation) of nanomaterials in the presence of an analyte (Le et al., 2014). In one such report, RNA aptamer-tagged AuNPs were employed to detect the avian influenza virus based on change in color of the nanoparticles due to aggregation (Le et al., 2014). The AuNPs conjugated with aptamers formed a shell around the virus envelope, indicating changes in size and density of the nanoparticles with a visual color change. The color-changing property of metal nanoparticles can also be coupled with enzyme-induced metallization for signal amplification (color) to achieve sensitive detection of target molecules (e.g., H9N2) (Zhou et al., 2014). The total assay time was reported to be approximately 1.5 h for detection of the H9N2 virus using this method. However, the developed color was sometimes too faint to be detected by the human eye. Precise instruments can be used to enhance sensitivity in such cases. For instance, a plasmon-assisted fluoro-immunoassay was explored for detection of an influenza virus (H3N2) using AuCNTs. The developed method offered a linear detection range of 50 to 10,000 PFU/

mL (detection limit of 50 PFU/mL) with an assay time of 1 h (Lee et al., 2015).

(ASOs) capped AuNPs (Moitra et al., 2020). The ASO-AuNPs interacted specifically with the target RNA (nucleocapsid phosphoprotein gene) sequence of SARS-CoV-2 to cause the agglomeration of AuNPs in infected patient's samples. The change in surface plasmonic properties of AuNPs in the presence of target gene sequence led to change in color of analyte solution. For further signal amplification, the RNaseH was added to the analyte mixture leading to development of a visually detectable precipitate. The developed sensor exhibited good selectivity (in the presence of MERS-CoV viral RNA), LOD of 0.18 ng/μL, and detection time of 10 min from the isolated RNA samples without the requirement of any sophisticated instrumental techniques.

Luminescence resonance energy transfer (LRET) has been applied to optical detection of the avian influenza virus (AIV). For example, energy transfer between BaGdF5:Yb/Er upconversion nanoparticles and AuNPs was used for sensitive and selective detection of AIV. Although the LRET-based biosensor offered a wide linear detection range (10 pM to 10 nM) with a detection limit of approximately 7 pM, the assay took nearly 2 h, which is quite time consuming (Kwon et al., 2014). The H1N1 virus has also been detected using a sandwich immunoassay based on autocatalytic activity of silver nanoparticles with a detection limit of 10^{-13} g/mL (Li et al., 2014). To develop the assay, H1N1 polyclonal antibodies were conjugated to silver nanoparticles (AgNPs) through an Ag-S bond. The sandwich-type immunoassay was performed on ELISA microtiter plates. After formation of an Ab/Ag/Ab-AgNP complex, 0.01 M nitric acid was added to dissolve the bound silver conjugates in solution and release Ag^{+} ions. Next, an o-phenylenediamine substrate was added to the wells and oxidized by Ag^{+} ions to fluorescence. The produced fluorescence was measured (Exct.365/Em.558 nm) and correlated with the concentration of antigens present in the assay medium (Li et al., 2014).

Another optical option involves surface-enhanced Raman spectroscopy (SERS). In this method, active Raman probe molecules are used for signal detection. The ability of SERS to provide rapid and sensitive detection of airborne analytes (Fang et al., 2014) was proven by detection of RSV using TMB as a Raman probe (shown in Fig. 5) (Zhan et al., 2016). Oxidation of TMB by horseradish peroxidase led to generation of TMB^{+}. The positively charged TMB ions adhered electrostatically to the negatively charged surface of AgNPs. Agglomeration of AgNPs thus caused, generated the SERS signal. The method was able to detect sub-picomolar levels of RSV (detection limit = 0.05 pg/mL) within a linear range of 0.5 to 20 pg/mL (Zhan et al., 2016).

Metal-enhanced fluorescence has also been used to detect airborne pathogens. For example, the recombinant hemagglutinin (rHA) protein of the H5N1 influenza virus was detected in human serum using aptamer-conjugated Ag@SiO_2 nanoparticles (Pang et al., 2015). Thiazole orange dye was used as a fluorescence probe to detect analytes. The system was able to detect rHA in both an aqueous buffer and human serum samples. A polyethylene tube was used as a detection platform to pave the way toward development of a point-of-care device. The sensor exhibited linear detection ranges of 2–100 ng/mL and 3.5–100 ng/mL in buffer and human serum samples, respectively, with an assay time of 30 min (Pang et al., 2015).

Similarly, SPR has been used extensively to detect airborne pathogens. For example, AuNP-alloyed quaternary l-cysteine-capped CdSeTeS quantum dots were employed for detection of H1N1 and H3N2 viral pathogens in 15–20 min (Takemura et al., 2017). The results indicated successful detection of H1N1 in deionized water and human serum. The developed method was also utilized in sensing of clinically isolated H3N2 and norovirus-like particles (Takemura et al., 2017). In another work, an SPR-based fluorescence-enhancement mechanism was utilized to detect norovirus-like particles using CdSe-ZnS-based quantum dots (Fig. 6). The detection limit of the developed sensor was 0.01 ng/mL (Ashiba et al., 2017).

Target-responsive hydrogel-based quantum dots have also been reported as fluorescent probes for fluorescence quenching–based detection of avian influenza virus (H5N1) (Xu et al., 2016). The linear range, in this case, was 2–1.2 to 26 hemagglutinating units per 20 μL, with an assay time of 30 min (Fig. 7).

In a novel approach, a Mach–Zehnder optical waveguide system was developed to detect H1N1/HA1 using antibody molecules within approximately 15 min (Sakamoto et al., 2016). EDC/NHS chemical crosslinking chemistry was used to immobilize antibody molecules on sol-gel glass for detection of analyte based on an optical output.

Aerobiological pathogen contamination in hospitals is a major healthcare challenge. Contaminants and pathogens can result in nosocomial infections capable of causing diseases that pose severe health risks. Detection tools for these contaminants in hospital environments are therefore urgently needed. In one study, evanescent-field fiber-optic sensor was employed to detect methicillin-resistant *Staphylococcus aureus* and *Streptococcus pneumoniae* within 6 and 13 h, respectively

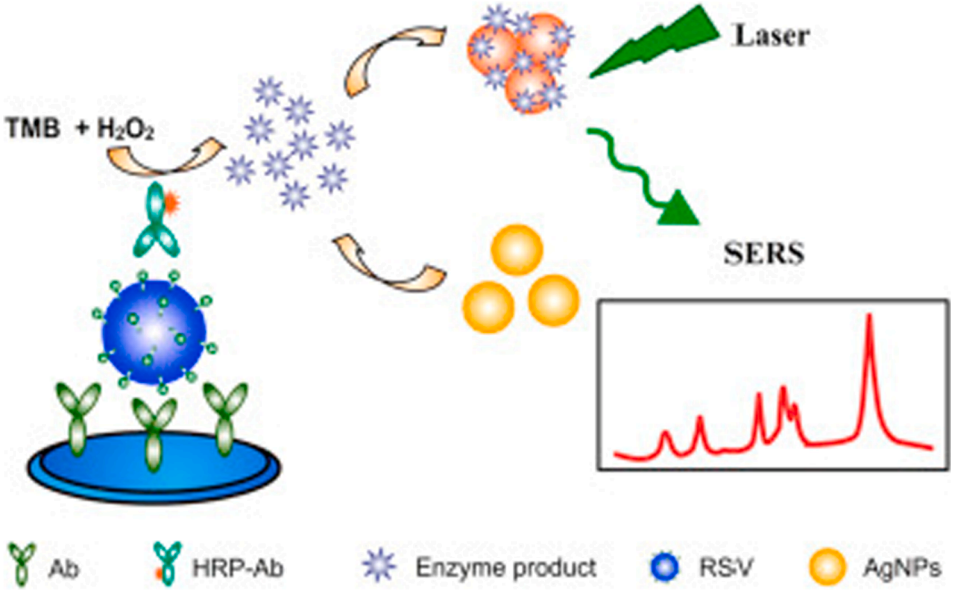

Fig. 5. SERS-based detection of RSV (Zhan et al., 2016).

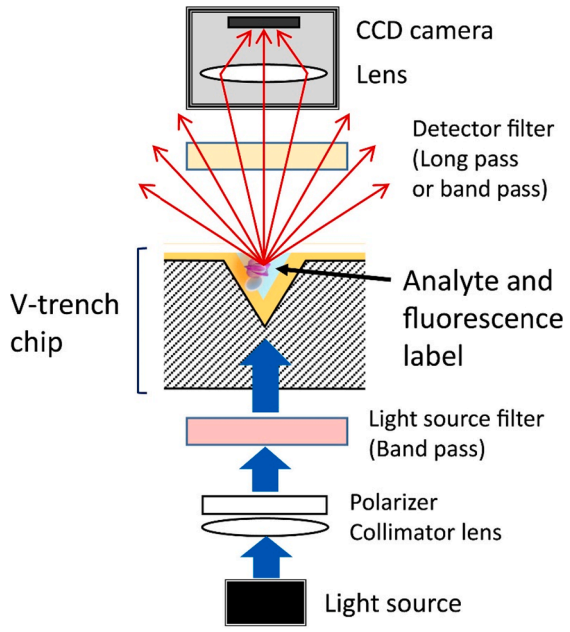

Fig. 6. Schematic for an SPR-based method for detection of norovirus-like particles. (Ashiba et al., 2017).

(Ferreira et al., 1999). The sensor consisted of an optical fiber connected to an air-sample collector through which sampled air passed onto a bacteria growth media. The evanescent coupling interactions occurred between the bacteria (in culture media) and the optical fiber (over the culture media), leading to optical attenuation. The attenuation is caused primarily by changes in the intrinsic absorption coefficient and refractive index of propagating light due to bacterial growth and enzymes released by bacteria, respectively (Ferreira et al., 1999). The decrease in optical power at the end of the fiber was therefore indirectly related to the number of bacteria present in sample volume.

In another study, a label-free optical biosensor based on reflectance measurements was constructed using three-dimensional SiO_2-based inverse opal nanostructures (Lee et al., 2018b). These nanostructures were conjugated with antibodies for specific binding to the target (H1N1 virus). Binding of the virus to the antibody-conjugated nanostructures caused a redshift of the reflectance peak that was measured and analyzed. The sensor offered high sensitivity and specificity toward H1N1 virus particles in the range of 10^3–10^5 PFU (Lee et al., 2018b).

Further, the recent occurrence of COVID-19 pandemic caused by the deadly virus (SARS-CoV2) has led to the development of several indirect detection assays using nanomaterials. The assays are based on the detection of antibodies against SARS-CoV2 in human serum samples (Chen et al., 2020; Wen et al., 2020). For instance, a lateral flow immunoassay (LFIA) was developed using lanthanide-doped polystyrene nanoparticles (LNPs) to detect anti-SARV-CoV-2 IgG in serum samples of infected humans within 10 min. The anti-SARV-CoV-2 IgG present in sample solutions interacted specifically with the nitrocellulose membrane immobilized recombinant nucleocapsid phosphoprotein to form an immunocomplex. Next, the secondary antibodies (mouse anti-human IgG antibody) labeled with LNPs were added to the analyte solution for the fluorescence based detection of anti-SARV-CoV-2 at excitation and emission wavelengths of 365 and 615 nm, respectively. The assay results were further validated using RT-PCR. The developed assay showed rapid and sensitive detection of anti-SARS-CoV-2 IgG in human serum samples of infected patients. The assay can also aid in monitoring the progression of COVID-19 and for evaluating the response of patients to the undergoing treatment (Chen et al., 2020).

In a similar report, AuNPs-based LFIA was developed for the detection of anti-SARS-CoV-2 IgM antibody in serum of COVID-19 positive patients (Huang et al., 2020). The anti-human IgM conjugated AuNPs were used as reporter molecules in the assay. In the presence of anti-SARS-CoV-2 IgM, the immunocomplex was formed at the capture membrane (SARS-CoV-2 nucleoprotein/Ig M). The developed complex was further detected using anti-human IgM/AuNPs with AuNPs based on the development of red color due to the aggregation of AuNPs on the test line of LFIA strip. The assay results were found to be comparable to the standard RT-PCR method with good sensitivity and specificity (κ coefficient = 0.872). Also, the assay could achieve the detection results within 15 min and low sample volumes (10–20 μL serum). The advantages associated with the developed LFIA (such as ease of operation, low cost, and rapid results) made them a viable method for the diagnosis of COVID-19 in clinical samples (Huang et al., 2020).

In addition, an LFIA-based combined antibody test (Ig M and Ig G) was also developed using AuNPs to diagnose the COVID-19 patients at different infection stages (Li et al., 2020). The AuNPs were conjugated with anti-IgM and anti-IgG human antibodies to form reporter molecules. The conjugates were further immobilized over assay strip at two respective detection zones (i.e., G and M). Upon addition of the sample containing anti-SARS CoV-2 IgG/IgM, the AuNPs conjugated with SARS CoV-2 antigen interacted with it at the conjugation pad to form an

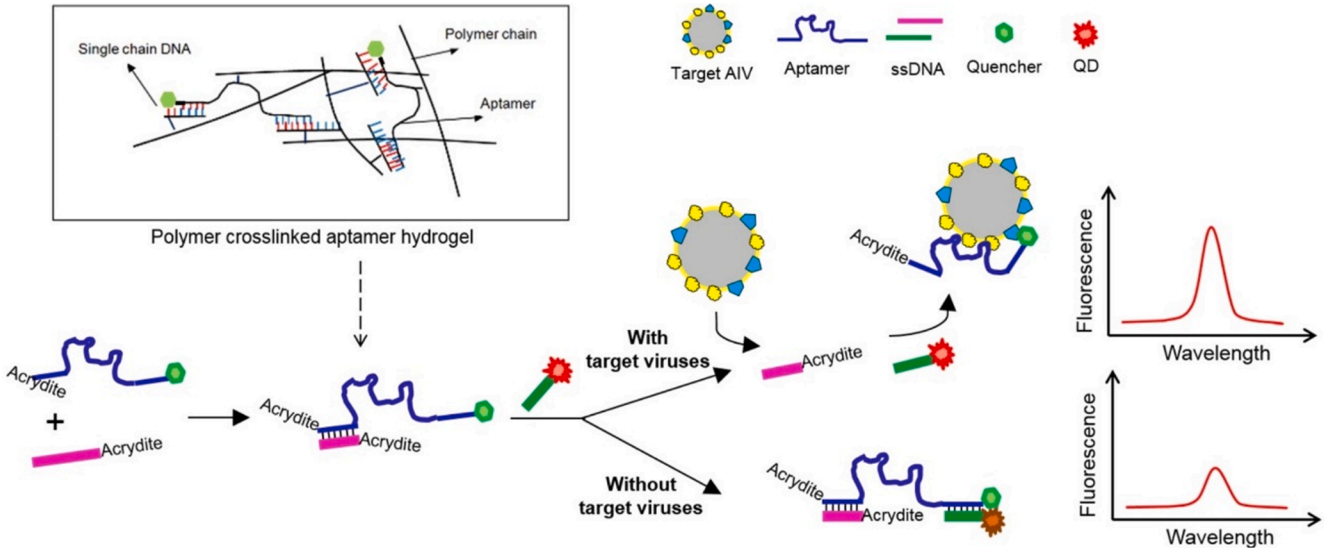

Fig. 7. Hydrogel embedded with quantum dots for detection of H5N1 (Xu et al., 2016).

immunocomplex. The developed immunocomplex containing solution further moves to the G and M test zones to combine with their respective secondary Abs conjugated with AuNPs to form visible red colored lines of detection (Fig. 8). The combined assay kit showed better results in terms of utility and sensitivity than that with a single IgM or IgG test. Other research group also reported a similar AuNP-based combined antibody assay kit for the detection of SARS-CoV-2 in whole blood and plasma samples (Pan et al., 2020). Also, selenium NPs-based LFIA strips have been reported for detection of IgM and IgG in plasma samples of COVID-19 suspected patients (Wang et al., 2020). The developed combined assay kits can be used for the rapid screening of SARS-CoV-2 carriers in the community (whether symptomatic or asymptomatic) and thus can help in the control of pandemic situation worldwide. However, the major limitation associated with these kits is that they cannot detect the acute infections to undertake the necessary actions. Also, the cross-reactivity with other human coronaviruses (e.g. common cold) can generate false results to limit their application for clinical use (https://www.who.int/news-room/commentaries/detail/advice-on-the-use-of-point-of-care-immunodiagnostic-tests-for-covid-19).

4.2. Electrochemical sensing of airborne pathogens

Although optical biosensors are relatively easy to construct and use, they can suffer from limited sensitivity and are not necessarily portable. Electrochemical sensors, on the other hand, can be designed to be more portable and sensitive and offer a fast response time. Electrochemical sensors rely on measurement of electrical signals arising from chemical changes due to binding of analytes to a transducer surface. Many electrochemical techniques (such as linear-sweep voltammetry [LSV], differential-pulse voltammetry [DPV], electrochemical impedance spectroscopy, conductometry, and amperometry) have been developed for detection of analytes. For example, chemiresistive biosensing electrodes based on probe DNA–conjugated CNTs were designed to detect H5N1 DNA sequences (Fu et al., 2017). The probe DNA–functionalized CNT electrodes could detect target DNA at concentrations ranging from 2 pM to 2 nM within 15 min (Fu et al., 2017). In another report, a label-free conductometric sensor was created to detect influenza virus (type A) using multi-walled carbon nanotubes (MWCNTs) (Tam et al., 2009). The sensor was developed by immobilizing DNA probes on the surface of the MWCNTs. Upon hybridization with target DNA, the DNA probes led to changes in the output signal. The sensor offered an assay time for influenza of approximately 4 min, with a detection limit in the nanomolar range (0.5 nM).

The potential differences arising from binding events can also serve as characteristic signals that can be exploited to detect sensitive biological interactions. DPV and LSV can both detect even small changes in the potential values. A DPV-based electrochemical sensor has been employed to detect H5N1 based on aptamer-conjugated MWCNT/polypyrrole nanowires/graphene nanoplatelets (Liu et al., 2011). In another work, an H1N1 immunosensor was built based on paper/stencil-electrodes modified with silica nanoparticles, single-wall carbon nanotubes (SWCNTs), and chitosan (Devarakonda et al., 2017). The researchers reported that their DPV-based immunosensor could achieve a detection limit of 113 PFU/mL for H1N1 and the system could be developed as an on-site diagnostic system. Also, a DPV-based dual immunosensor has been developed using methylene blue (MB)–electroadsorbed graphene oxide nanostructures for detection of H5N1 and H1N1. The electrochemically adsorbed MB molecules over graphene oxide–modified electrodes exhibited high electron-transfer properties for biomolecular recognition. Chitosan and protein A molecules were also employed as interface layers for fabrication of a sensor. The chitosan molecules had a multifunctional role in designing the biosensor due to their solubility in mildly acidic aqueous solutions, film-forming ability, electroconductivity, and presence of functional groups for cross-linking interactions. Protein A promoted oriented immobilization of antibodies, allowing free F_{ab} regions of bound antibodies to interact with the epitopes of target antigens (Fig. 9). The developed sensor provided good sensitivity in the picomolar range (25–500 pM) and short response time (<1 min) (Veerapandian et al., 2016). Aptamer-

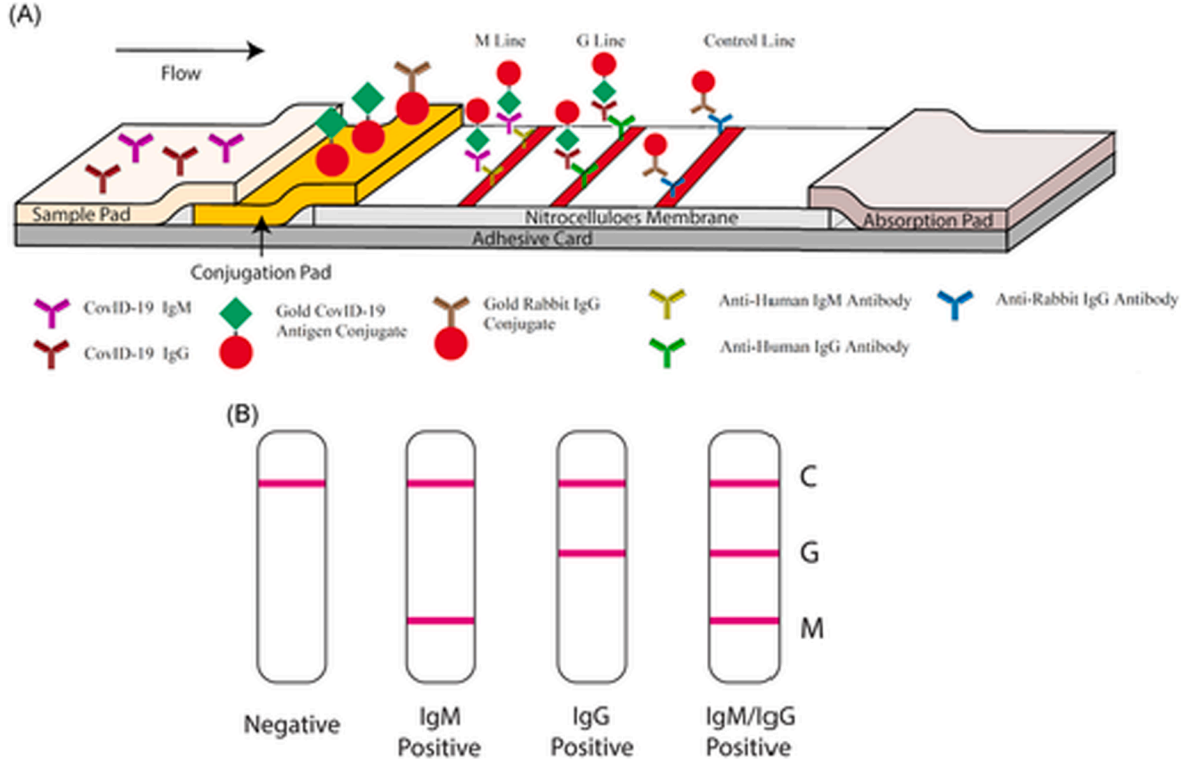

Fig. 8. (A) Schematic of rapid SARS-CoV-2 IgM-IgG combined antibody kit using AuNPs; (B) Illustration of different testing results (Li et al., 2020).

conjugated AuNPs decorated over screen-printed carbon electrodes were employed for DPV-based detection of H5N1 (Diba et al., 2015). The authors reported the lowest detectable limits of H5N1 virus at a femtomolar concentration (100 fM) over a linear dynamic detection range of 100 fM to 10 pM.

LSV has also been used for detection of airborne pathogens. For example, an AuNP-graphene nanocomposite (bound to polyclonal antibodies) was used as a tracer label for quantification of avian influenza virus H7 (AIV H7) in a sandwich assay format (Huang et al., 2016). In the assay, AuNP-graphene nanocomposites modified gold electrodes labeled with modified antibodies (mAbs) were used to capture target antigens. Next, surface-bound viral antigens were incubated with a polyclonal antibody (pAb)-AgNP/graphene composite to form a sandwich complex for LSV-based detection. The developed sandwich-type immunosensor offered a detection limit of 1.6 pg/mL due to amplification of the signal using AgNPs (Huang et al., 2016). In another work, detection of H1N1 and norovirus was reported using Au/magnetic nanoparticle (MNP)-CNTs deposited over platinum inter-digited electrodes (Lee et al., 2018a). The Au/MNP-CNTs were conjugated with probe DNA molecules for hybridization with target analytes to cause changes in conductivity, as measured by LSV (Fig. 10). The detection limits of this sensor for H1N1 and norovirus were estimated at 8.4 and 8.8 pM, respectively (Lee et al., 2018a). A highly sensitive electrochemical biosensor based on a digital enzyme-linked immunoassay was reported for detection of H7N9 avian influenza virus with a detection limit of 7.8 fg/mL (Wu et al., 2018). The sensor was developed by combining bifunctional fluorescence magnetic nanospheres (bi-FMNs) with mAb-AuNP modified microelectrode arrays. The FMNs were conjugated to pAbs and an alkaline phosphatase (ALP) enzyme to separate the H7N9 particles from complex samples. The target-bound bi-FMNs were later added to the AuNP-bound microelectrode arrays to form a sandwich complex (ALP-FMNs-Ab/Ag/Ab-AuNP). Phosphorylation of p-aminophenyl phosphate monohydrate resulted in production of p-aminophenol (p-AP). In the next step, the generated p-AP was able to induce reduction of Ag^{+} to Ag^{0} form. The Ag^{0} was later deposited over microelectrode arrays and measured by LSV (Wu et al., 2018). A similar detection platform based on oligonucleotide-modified gold electrodes was proposed to detect the cDNA of H5N1 based on square-wave voltammetry (Grabowska et al., 2013).

Amperometry is a technique in which the changes in current in response to biological events are recorded by sensing applications (Dong et al., 2015). In this context, chronoamperometry was employed for label-free detection of H1N1 with the aid of reduced graphene oxide (GO) coupled with a microfluidics platform (Singh et al., 2017). Microelectrodes containing micro channels were fabricated on a glass substrate through which the sample was allowed to flow (Fig. 11). The electrochemical approaches allowed for high selectivity and sensitivity (Singh et al., 2017). DNA can also be used as a probe for sensing purposes. In this context, DNA tetrahedral probes have been explored for electrochemical detection of H7N9 (Dong et al., 2015). An amperometric signal was generated when a complementary single-stranded DNA was bound to its target sequence, converting TMB to an oxidized state. The amperometric signal was proportional to the concentration of virus particles in the test solution. This sensitive method could detect virus particles at a level of 100 fM and was not affected by the presence of potentially interfering viruses (Dong et al., 2015).

Impedance-based methods are commonly used electrochemical techniques (Jarocka et al., 2014; Karash et al., 2016). Variation in impedance signal is used to detect almost all airborne pathogens. This principle was applied to detection of H5N1 based on MWCNT–cobalt phthalocyanine– polyamidoamine nanocomposite (Zhu et al., 2009). This impedance-based sensing method has also been used to detect Der p2 antigens based on AuNPs (Bau and Wang 2011; Chen et al., 2012; Tsai et al., 2011), H5N1 based on an aptasensor with AuNPs and carbon (Jarocka et al., 2014; Karash et al., 2016), Der p2 antigens based on AuNPs on a polycarbonate substrate (Shen et al., 2017), and Der p2 allergens based on AgNPs deposited on a AuNP layer (Liu et al., 2012). A screen-printed GO textile–based material tested for impedimetric detection of influenza virus (Kinnamon et al., 2018) was found to be an inexpensive and wearable point-of-exposure method. Printing was performed on polyamide and textile materials that were later immobilized with antibodies against H1N1 virus. With antigen and antibody interactions, H1N1 was detected using electrochemical impedance spectroscopy (EIS) (Kinnamon et al., 2018). As with this flexible electrode, the potential of on-chip integrated rolled-up nanomembrane DNA-based electrodes was also studied for label-free sensing of H1N1 viruses. The EIS-based method was sensitive to target viruses, with a detection limit of 20 aM (Medina-Sánchez et al., 2016).

Field-effect transistors (FETs) are another important category of electrochemical biosensors. The high sensitivity of FET-based sensors is highly advantageous compared with other nanomaterial-based electrochemical sensors. In addition, the FET-based nanosensors can be developed at large scales due to ease of mass production with good portability and versatility (Syedmoradi et al., 2019). Several nano-FET biosensors have been developed using silicon nanowires (SiNWs), carbon nanotubes (CNTs), graphene, metal oxide, and transition metal dichalcogenide-based (TMDs) with high sensitivity and faster detection times. For example, CNT-based FETs can detect influenza A virus DNA at picomolar concentrations and offer a prolonged shelf life, producing a 97% output signal even after 7 months of storage (Tran et al., 2017). In another study, a group of researchers used SWCNTs to detect H5N1 based on the FET approach (Thu et al., 2013). The authors were also able

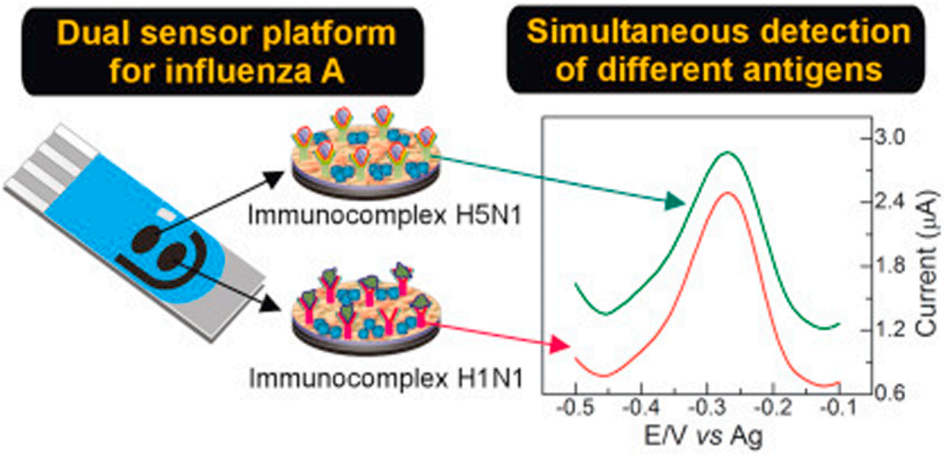

Fig. 9. Dual-sensor platform for simultaneous detection of influenza virus antigens (Veerapandian et al., 2016).

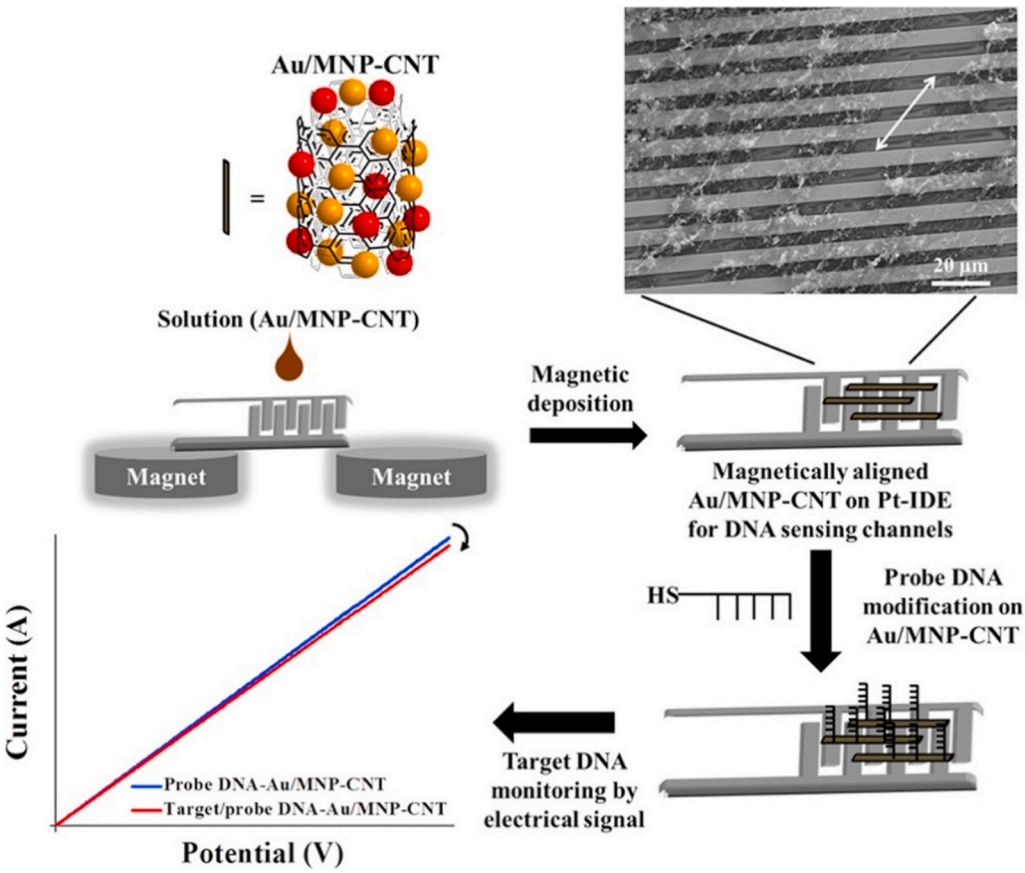

Fig. 10. Detection of H1N1 virus using Au/MNP-CNTs employing a linear sweep voltammetry technique (Lee et al., 2018a).

to detect the virus at picomolar concentrations. However, an assay time greater than 1 h limits use for rapid detection of microbes. As an alternative, indium tin oxide (ITO) thin films have been used to detect airborne pathogens. Guo et al. (2013) used monoclonal antibodies to decorate an ITO channel for detection of H5N1 using (3-glycidoxypropyl) trimethoxysilane. Although it was able to sense the virus selectively, its nanomolar linear range of detection was low relative to the picomolar range of other reported sensors (Guo et al., 2013). Silicon nanowires (SiNWs) have also been explored as FET-based platforms for detection of airborne analytes. For example, SiNW-FETs were designed to determine H1N1 DNA sequences (Karnaushenko et al., 2015). The detection limit of the system for H1N1 was in the picomolar range and an output signal was obtained within 30 min. In another work with SiNWs, the influenza A virus was detected at levels as low as 29 viruses/μL in clinically exhaled breath condensate samples (Fig. 12) (Shen et al., 2012). The impaction on a gel approach was used to collect viruses for their optical detection (Ferreira et al., 1999). This sampler mainly consisted of vacuum pump (flow rate of 1001 min^{-1}), perforated plates, and agar containing Petri plates. This sampler was arranged in a way that the air containing particles < 10 μm were directly diverted to the agar containing Petri plates. For the sensing of SiNW-based sensing of H1N1 virus, a device for collecting exhaled breath condensate (EBC) was used as a sampler to collect virus particles (Shen et al., 2012). In general, ECB was composed of four parts, (1) and (2) collection device cover and base, (3) ice layer, and (4) −70 °C treated hydrophobic layer. A hole in the device cover was used for the inlet of exhaled breath, while the ice layer was used to cool the hydrophobic layer. The low temperature of the hydrophobic layer (parafilm) led to immediate condensation of the inlet air in the form of small droplets. The condensed droplets were then recovered using DI water to detect the presence of viruses. The authors also reported high selectivity of the proposed system even in the presence of H1N1 influenza virus, 8 iso PGF 2a biomarkers, and other interferents.

Recently, a graphene-based FET immunosensor was reported for the detection of SARS-CoV-2 in nasopharyngeal swab samples (Seo et al., 2020). The aqueous solution gated FET sensor consisted of a SARS-CoV-2 antibody conjugated graphene channel covered with an electrolyte (phosphate-buffered saline; pH 7.4). The changes in channel surface potential in the presence of SARS-CoV-2 and the corresponding effects on the gated voltage were measured and correlated to the antigen concentration. The developed FET sensor against SARS-CoV-2 showed LOD of 1.6×10^1 pfu/mL and 2.42×10^2 copies/mL in culture medium and clinical samples, respectively without any sample pretreatment. In addition, the sensor showed good specificity towards SARS-CoV-2 proteins when tested in the presence of MERS-CoV proteins. Thus, the FET sensor can be a great tool for real time detection of virus in clinical samples.

5. Performance evaluation of sensing techniques

The limitations of conventional sensing techniques for quantitation of airborne pathogens have been described in a number of respects. The performance of those systems is often undesirable in many respects (e.g., non-portability, delayed response, non-specific response, and below-par sensitivity). In an effort to resolve such limitations, use of nanomaterials has been proposed as one of the best available options, particularly for fabricating a reliable, rapid, automated, and sensitive sensor. A number of nanomaterials have been employed to improve speed and sensitivity over an extended range of concentrations for diverse pathogens (Table 1). Depending upon the type of material and sensor, the performance of nanomaterials can vary. In many cases, full information on sensor performance metrics is not provided by the authors. We therefore confined our comparison of performance to a few key variables (detection limit, linear working range, and detection time) between airborne

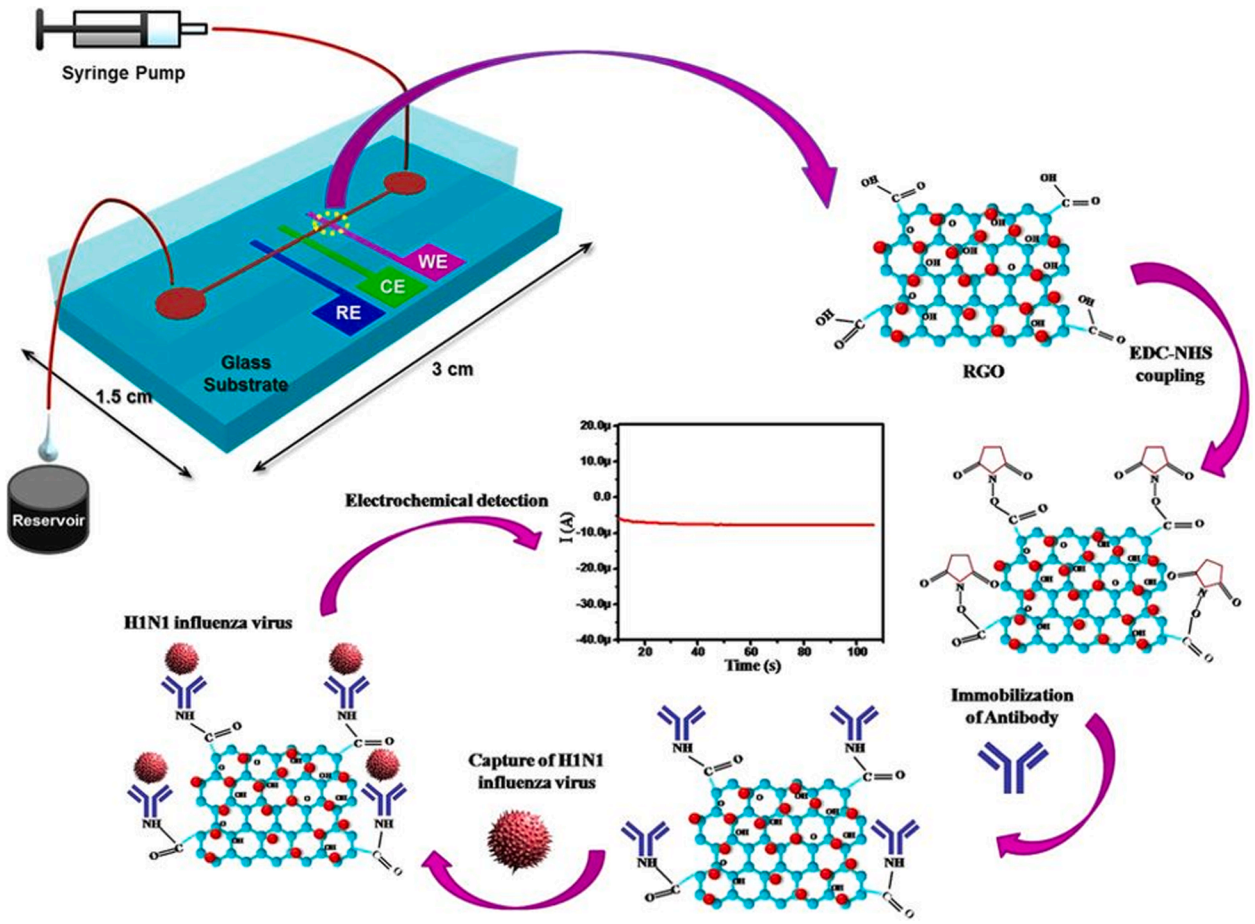

Fig. 11. Schematic for reduced graphene oxide nanostructure–based immune sensor integrated with microfluidics for detection of H1N1 (Singh et al., 2017).

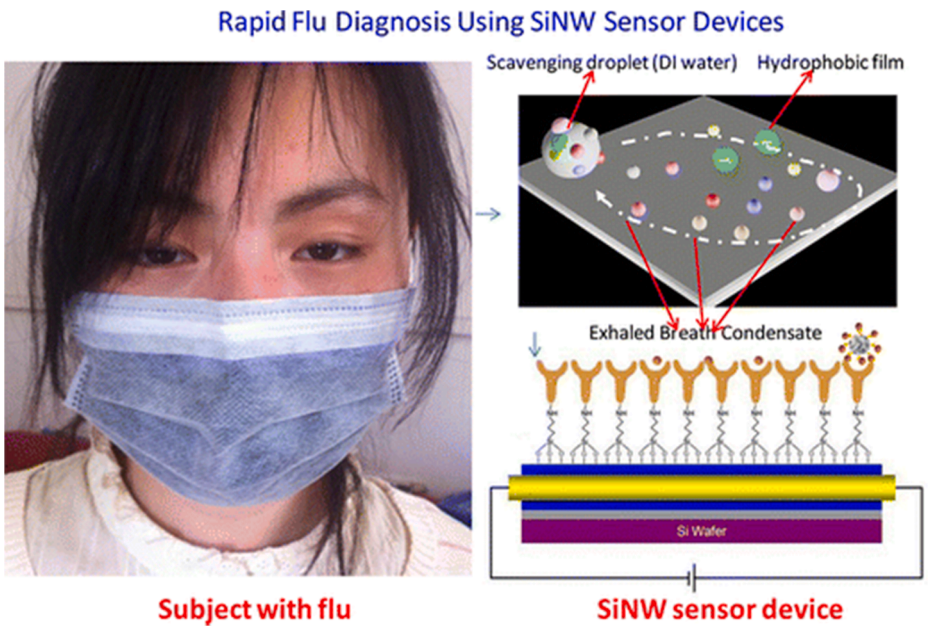

Fig. 12. Silica nanowire-based sensor for influenza A virus detection (Shen et al., 2012).

pathogen sensing devices.

The optical as well electrochemical properties of nanomaterials have been explored to build efficient detection systems. However, a direct comparison of the performance of these sensors cannot be made on a parallel basis due to the different methodologies adopted for determination of pathogens. Nonetheless, the sensitivities of both types of sensors displayed large variabilities according to type of analyte pathogen. For the H5N1 influenza virus, an electrochemical sensor comprising

Table 1
Evaluation of various sensing parameters of differnet optical and electrochemical sensors for airborne pathogens.

S. No.	Nanomaterial/detection technique	Target	Linear range	Detection limit	Detecti on time (min)	Reference
Optical detection						
	Au-CNT nanohybrid/ colorimetric	H3N2 influenza virus	10–50000 PFU/mL	3.4 PFU/mL	10	(Ahmed et al., 2016)
	Grp-Au NP hybrids/ colorimetric	Norovirus-like particles	100 pg/mL–10 μg/mL	92.7 pg/mL	5	(Ahmed et al., 2017)
	AuNPs–GO hybrids/ colorimetric	Respiratory syncytial virus (RSV)	0.1–10 pg/mL	0.04 pg/mL	20	(Zhan et al., 2014)
	RNA conjugated AunNPs/ colorimetric	Influenza virus	–	–	–	(Le et al., 2014)
	AuNPs/colorimetric	H9N2 avian influenza virus	0.1–1000 ng/mL	17.5 pg/mL	90	(Zhou et al., 2014)
	AuCNTs/fluoro-immunoassay	H3N2 influenza virus	50–10,000 PFU/mL	50 PFU/mL	60	(Lee et al., 2015)
	AgNPs/luminescence resonance energy transfer	H1N1 influenza virus	1 pg/mL– 10 ng/mL	0.1 pg/mL	120	(Fang et al., 2014)
	AgNPs/surface-enhanced Raman spectroscopy	RSV	0.5–20 pg/mL	0.05 pg/mL	10	(Zhan et al., 2016)
	$Ag@SiO_2$ nanoparticles/metal enhanced fluorescence	H5N1 influenza virus	2–100 ng/mL (buffer) and 3.5–100 ng/mL (human serum)	2 and 3.5 ng/mL	30	(Pang et al., 2015)
	AuNP-CdSe/TeS-QDs alloyed/ surface plasmon resonance	H1N1 and H3N2 influenza virus		0.03 pg/mL (DI), 0.4 pg/ mL (human serum) and 10 PFU/mL	15–20	(Takemura et al., 2017)
	CdSe-ZnS-QDs/Surface plasmon resonance	Norovirus-like particles	–	0.01 ng/mL	–	(Ashiba et al., 2017)
	CdSe/ZnS QDs/Fluorescence quenching	H5N1 avian influenza virus	$2^{-1.2}$–2^{6} HAU per 20 μL	0.4 HAU	30	(Xu et al., 2016)
Electrochemical detection						
	CNTs/chemiresistive sensing	H5N1 influenza virus	2 pM–2 nM	2 pM	15	(Fu et al., 2017)
	MWCNTs/conductometric sensing	Influenza virus (type A)	1–10 nM	0.5 nM	4	(Tam et al., 2009)
	MWNT/PPNWs/GNPs/ differential-pulse voltammetry	H5N1 avain influenza virus	5.0×10^{-12}– 1.0×10^{-9} M	4.3×10^{-13} M	–	(Liu et al., 2011)
	SWCNT/differential-pulse voltammetry	H1N1 influenza virus	1–10^4 PFU/mL	113 PFU/mL	30	(Devarakonda et al., 2017)
	GO nanostructures/differential-pulse voltammetry	HA proteins of H5N1 and H1N1 influenza virus	25–500 pM	8.3 pM	< 1	(Veerapandian et al., 2016)
	AuNPs/differential-pulse voltammetry	H5N1 avian influenza virus	100 fM–10 pM	100 fM	–	(Diba et al., 2015)
	AgNPS-G/linear-sweep voltammetry	avian influenza virus H7	1.6×10^{-3}–16 ng/mL	1.6 pg/mL	30	(Huang et al., 2016)
	Au/MNP-CNTs/linear-sweep voltammetry	H1N1 influenza virus and norovirus	1 pM–10 nM	8.4 and 8.8 pM	–	(Lee et al., 2018a)
	bi-FMNs-AgNPs/linear-sweep voltammetry	H7N9 avian influenza virus	–	7.8 fg/mL	–	(Wu et al., 2018)
	rGO/amperometry	H1N1 influenza virus	1–10^4 PFU/mL	0.5 PFU/mL	2	(Singh et al., 2017)
	MWNTs–CoPc/electrochemical impedance spectroscopy	H5N1 avian influenza virus	0.01–500 ng/mL	1.0 pg/mL	–	(Zhu et al., 2009)
	AuNPs/electrochemical impedance spectroscopy	Der p2 allergen	27.5–400 ng/mL	16.47 ng/mL	–	(Shen et al., 2017)
	AuNPs/electrochemical impedance spectroscopy	Der p2 allergen	1 μg/mL–10 pg/mL	10 pg/mL	~120	(Liu et al., 2012)
	GO/electrochemical impedance spectroscopy	H1N1 influenza virus	10 ng/mL–10 μg/mL	10 ng/mL	>47	(Kinnamon et al., 2018)
	Rolled-up nanomembrane/ electrochemical impedance spectroscopy	H1N1 avian influenza virus	20 aM–2 pM	20 aM	–	(Medina-Sánchez et al., 2016)
	CNTs/field-effect transistors	influenza A virus	1 pM–10 nM	1 pM	1	(Tran et al., 2017)
	SWCNTs/field-effect transistors	H5N1 avian influenza virus	100 pM–1 nM	1.25 pM	–	(Thu et al., 2013)
	ITO thin films/field-effect transistors	H5N1 avian influenza virus	5 ng/mL–5 μg/mL	0.08 ng/mL		(Guo et al., 2013)
	SiNWs/field-effect transistors	H1N1 avian influenza virus	40–100 pM	40 pM	30	(Karnaushenko et al., 2015)
	SiNWs/field-effect transistors	Influenza virus H3N2	–	29 viruses/μL	>1	(Shen et al., 2012)

MWCNT–CoPc was far more sensitive than optical sensors based on an $Ag@SiO_2$ nanoparticle developed for the same analyte (Pang et al., 2015; Zhu et al., 2009). An electrochemical sensor was sensitive enough to achieve a detection limit of 1 pg/mL for H5N1, while an optical sensor was able to detect the same target at 2000 pg/mL. The MWCNT–CoPc exhibited excellent sensitivity for H5N1 due primarily to a high conjugation capacity for the recognition probe and improved oxidation signals (Zhu et al., 2009). In contrast, the optical sensor (based on AgNPs) developed for H1N1 influenza virus was 100,000 times more sensitive than electrochemical sensors (based on GO) in terms of detection limits

(Fang et al., 2014; Kinnamon et al., 2018). The fluorescence reaction of Ag^+ autocatalysis was speculated to be the key explanation for the high sensitivity of an AgNP-based optical sensor (Fang et al., 2014). The Ag^+ was generated from AgNP labels attached to antibodies.

In detection of particular pathogens, an optical sensor developed using an Au-CNT nanohybrid was found to be excellent in terms of sensitivity (Ahmed et al., 2016). It could detect H3N2 (whole virus particles) down to 3.4 PFU/mL, which was the lowest detection limit among sensors built for similar measurements. The detection limit of the Au-CNT nanohybrid-based optical sensor was 385 and 500 times better than those of the ELISA and commercial immunochromatography kits, respectively. This sensor was also able to sense airborne pathogens within 10 min. The performance of the optical sensor developed using AuNP–GO hybrids was also remarkable in terms of lower detectable concentration of RSV (Zhan et al., 2014). However, despite an excellent detection limit (0.04 pg/mL) and moderately good sensing time (e.g., 20 min), its application was limited in a broad sense due to its poor ability to maintain linearity over a wider range of RSV (e.g., 0.1–10 pg/mL). AgNPs are promising tools for improving sensing time (e.g., 10 min) and linear detection range (e.g., 0.1–20 pg/mL) in the form of an RSV optical sensor. Nonetheless, this AgNP-based RSV system involves a slight compromise on sensitivity compared with AuNP-based counterparts (Zhan et al., 2016) with a detection limit of 0.05 pg/mL. AgNPs are also effective for fabricating a sensitive sensor for H1N1 (Fang et al., 2014). However, a high detection time (120 min) reduced this sensor ranking on a list of the best performers. The detection time for H1N1 can be improved within 20 min using a AuNP-CdSe/TeS quantum dot alloy in an optical sensor (Takemura et al., 2017). Likewise, single-walled nanotubes (SWNTs) (Devarakonda et al., 2017) and reduced GO (Singh et al., 2017) were equally effective in terms of providing linear detectable electrochemical signals for H1N1. However, the superior electrochemical properties of reduced GO made it possible to achieve a lower detection limit (0.5 PFU/mL) and time (2 min). The detection limit and detection/incubation time achieved by SWNTs were 113 PFU/mL and 30 min, respectively. Overall, the nanomaterials displayed excellent performance in terms of fabricating rapid, specific, and sensitive sensors for detection of airborne pathogens.

In terms of the response time of the sensing systems for airborne pathogens, graphene-AuNP hybrids (Ahmed et al., 2017) and GO nanostructures (Veerapandian et al., 2016) were the most suitable to develop optical and electrochemical sensors, respectively. The corresponding time needed by these sensors was 5 and <1 min for determination of varying levels of norovirus-like particles and hemagglutinin proteins of H5N1/H1N1 influenza virus. In graphene-AuNP hybrid-based norovirus-like particle sensors, the excellent peroxidase-like activity of graphene-AuNP hybrids and their ability to conjugate more recognition molecules were postulated to be responsible for the rapid and sensitive detection (Ahmed et al., 2017). Moreover, the sensor also displayed a remarkable detection limit of 92.7 pg/mL, which was 112 times more sensitive than the most popular ELISA technique. Likewise, the superior electrochemical properties of electrodes modified by GO, MB, antibodies, chitosan, and protein-A structures provided excellent platforms for fabrication of extremely fast and sensitive sensors for HA proteins of H5N1 and H1N1 (Veerapandian et al., 2016). In addition to the superiority offered in terms of rapid detection, this electrochemical sensor was efficient enough to reach a detection limit of 8.3 pM.

In addition to these sensors, the optical sensors developed using AgNPs (Fang et al., 2014; Zhan et al., 2016), Ag@SiO_2 nanoparticles (Pang et al., 2015), AuNP-CdSe/TeS quantum dot alloys (Takemura et al., 2017), and CdSe/ZnS quantum dots (Xu et al., 2016) are also rapid enough to provide sensing signals within 30 min. However, nanomaterials offered more efficient options for rapid determination of airborne pathogens through electrochemical sensing. Nanomaterials such as MWCNTs (Tam et al., 2009), reduced GO (Singh et al., 2017), CNTs (Tran et al., 2017), and silicon nanowires (Karnaushenko et al., 2015) are efficient enough to determine airborne pathogens within 5 min. Moreover, the overall average time needed by the optical and electrochemical sensors listed in Table 1 is 39.5 min (between 5 and 120 min) and 25.5 min (between 1 and 120 min), respectively. On the basis of average time needed by the nanomaterial-based sensors, electrochemical sensors are faster than optical sensors. Particularly, the FET-based nanosensors have shown quick results with good reproducibility (Shen et al., 2012). The condensed breath droplets were directly used for FET-based detection of influenza flu virus using silica nanowires. Such sensors can also play a major role towards rapid detection of airborne pathogens (such as SARS COV-2) during pandemic conditions (Seo et al., 2020). Also, the FET-based nanosensors provided several advantages such as portability, ease of mass production, rapid results, and low cost analysis of air-borne pathogens (Syedmoradi et al., 2019). However, it is difficult to confine Ab and Ag molecules on the nanoscale wires to limit the mass production of FETs. An additional microfluidic system is thus required for stable immobilization of the Ab and Ag molecules on the nanoscale wires. However, such addition may lead to increase in cost of the developed FET sensors.

6. Conclusion and future prospects

The transmission of pathogens through the air in the form of liquid droplets, dust particles, spores, or combination of these forms has been recognized as a major problem worldwide. The pathogens may enter the air through diverse routes (coughing, sneezing, breathing, or even speaking from an infected individual). They can also be aerosolized from bodily fluids (blood or fecal matter) or environmental surfaces. Exposure to airborne pathogens can lead to several health problems (and economic losses) in the form of allergies, disorders, and miscellaneous diseases. A myriad of conventional options exists for detection of airborne pathogens, including culture-based colony-counting, immunological methods, and the molecular methods described in the current review. However, these methods detect pathogens mainly through indirect samples (such as nasal swabs and blood) that require time-consuming procedures.

Biosensors have recently emerged as efficient platforms for direct detection of pathogens in air. Microfluidic assays have been developed for the same purpose. Advances in nanomaterials and their outstanding sensing properties (especially high surface-area-to-volume ratio) have facilitated expansion of their application to various purposes. Nanomaterial-based optical and electrochemical biosensors have enabled the development of highly sensitive, miniaturized, portable, and rapid diagnostic systems for various bacterial and viral pathogens. The critical steps involved in detection of airborne pathogens are sample collection and interfacing of the sampling chamber with the diagnostic system. The air samples are collected using either filtration-based collectors (such as button air samplers, porous-membrane filters, and particle-to-liquid samplers) or gravitation-based collectors (such as impactors, aerosol centrifuges, and impingers). The main obstacle in sample collection is the need for highly sensitive collectors or sensors that can detect the low levels of pathogens found in air. In addition, the presence of interferents (e.g., dust particles or other pathogenic species) in the sample may clog air samplers and restrict collection (or identification) of the target pathogens from captured samples. The samplers can be positioned at suitable places to maximize capture of pathogens with minimum dust. The positioning of a sampler is important as the size of the particles in air greatly affects their travel distance. For example, larger particles ($d > 100$ μm) settle fast, whereas smaller particles ($d <$ 10 μm) remain suspended in the air with the target pathogens (viruses, bacteria, and spores).

The use of advanced nanomaterials in biosensing of airborne pathogens can greatly assist in providing a solution to the problems of low sensitivity and portability and ultimately allow the assembly of point-of-care air diagnostic systems. However, direct and automated interfacing of samplers with the detector (or probe) of sensing system is difficult to establish in portable, accurate, and on-site diagnostic systems. To date, a

number of companies have developed automated pathogen detection systems, including the CANARY Biosensor, BioHawk and Tac BioHawk, and Battelle Resource Effective Bio-Identification system for commercial sales and homeland security applications. However, use of these systems is also limited as they are not yet efficient enough for on-site diagnosis of pathogens due to their non-portability, expensiveness, and lack of interfacing with smart technology. The future works may be focused towards the development of breath samplers coupled with a nanosensor for rapid and *in-situ* detection of airborne pathogens. Also, the efforts should be made towards the mass production of nanosensors with good reproducibility and repeatability in the form of LFIA, FET biosensors, or microfluidic assays for commercial applications. Hence, further advances are needed for the development of an efficient and effective air-pathogen biosensing system with automated rapid sampling, high sensitivity, affordability, stability, and real-time and in situ detection of analytes.

Declaration of Competing Interest

The authors declare that they have no known competing financial interests or personal relationships that could have appeared to influence the work reported in this paper.

Acknowledgments

The corresponding author (KHK) acknowledges support made in part by a grant from the National Research Foundation of Korea (NRF) funded by the Ministry of Science, ICT, and Future Planning (Grant No: 2016R1E1A1A01940995). AD thanks the Department of Science and Technology (DST, India) for project grant (EMR/2016/006480; GAP-397) for project funding.

References

Agranovski, I.E., 2007. Personal sampler for viable airborne microorganisms: main development stages. CLEAN – Soil, Air Water 35, 111–117.
Agranovski, I.E., Safatov, A.S., Sergeev, A.A., Pyankov, O.V., Petrishchenko, V.A., Mikheev, M.V., Sergeev, A.N., 2006. Rapid detection of airborne viruses by personal bioaerosol sampler combined with the PCR device. Atmos. Environ. 40, 3924–3929.
Ahmed, S.R., Kim, J., Suzuki, T., Lee, J., Park, E.Y., 2016. Enhanced catalytic activity of gold nanoparticle-carbon nanotube hybrids for influenza virus detection. Biosensors Bioelectron. 85, 503–508.
Ahmed, S.R., Takemeura, K., Li, T.-C., Kitamoto, N., Tanaka, T., Suzuki, T., Park, E.Y., 2017. Size-controlled preparation of peroxidase-like graphene-gold nanoparticle hybrids for the visible detection of norovirus-like particles. Biosensors Bioelectronics 87, 558–565.
Alvarez, A.J., Buttner, M.P., Toranzos, G.A., Dvorsky, E.A., Toro, A., Heikes, T.B., Mertikas-Pifer, L.E., Stetzenbach, L.D., 1994. Use of solid-phase PCR for enhanced detection of airborne microorganisms. Appl. Environ. Microbiol. 60, 374–376.
Anderson, R.M., Fraser, C., Ghani, A.C., Donnelly, C.A., Riley, S., Ferguson, N.M., Leung, G.M., Lam, T.H., Hedley, A.J., 2004. Epidemiology, transmission dynamics and control of SARS: the 2002–2003 epidemic. Philos. Trans. R. Soc. London. Series B: Biol. Sci. 359, 1091–1105.
Angelakis, E., Yasir, M., Azhar, E.I., Papadioti, A., Bibi, F., Aburizaiza, A.S., Metidji, S., Memish, Z.A., Ashshi, A.M., Hassan, A.M., Harakeh, S., Gautret, P., Raoult, D., 2014. MALDI-TOF mass spectrometry and identification of new bacteria species in air samples from Makkah, Saudi Arabia. BMC Res. Notes 7, 892.
Ashiba, H., Sugiyama, Y., Wang, X., Shirato, H., Higo-Moriguchi, K., Taniguchi, K., Ohki, Y., Fujimaki, M., 2017. Detection of norovirus virus-like particles using a surface plasmon resonance-assisted fluoroimmunosensor optimized for quantum dot fluorescent labels. Biosensors Bioelectron. 93, 260–266.
Atreya, C., Mohan, K., Kulkarni, S., 2004. Rubella virus and birth defects: molecular insights into the viral teratogenesis at the cellular level. Birth Defects Res. Part A: Clin. Mol. Teratol. 70, 431–437.
Augustowska, M., Dutkiewicz, J., 2006. Variability of airborne microflora in a hospital ward within a period of one year. Ann. Agric. Environ. Med. 13, 99–106.
Bau, I.J., Wang, G.-J., 2011. A Highly Sensitive Electrochemical Impedimetric Nanobiosensor for Dust Mite Antigen Der p2 Detection, 3–9.
Baumgardner, D., Paretsky, D., 1999. The in vitro isolation of Blastomyces dermatitidis from a woodpile in north central Wisconsin, USA. Med. Mycol. 37, 163–168.
Burge, H.A., Solomon, W.R., 1987. Sampling and analysis of biological aerosols. Atmos. Environ. (1967) 21, 451–456.
Cao, G., Noti, J., Blachere, F., Lindsley, W., Beezhold, D., 2011. Development of an improved methodology to detect infectious airborne influenza virus using the NIOSH bioaerosol sampler. J. Environ. Monit. 13, 3321–3328.
Chakraborty, S., Kumar, N., Dhama, K., Verma, A.K., Tiwari, R., Kumar, A., Kapoor, S., Singh, S.V., 2014. Foot-and-mouth disease, an economically important disease of animals. Adv. Anim. Vet. Sci 2, 1–18.
Chantong, W., Kaneene, J.B., 2011. Poultry raising systems and highly pathogenic avian influenza outbreaks in Thailand: the situation, associations, and impacts. Southeast Asian J. Trop. Med. Public Health 42, 596.
Chen, Y.-S., Wu, C.-C., Tsai, J.-J., Wang, G.-J., 2012. Electrochemical impedimetric biosensor based on a nanostructured polycarbonate substrate. Int. J. Nanomed. 7, 133–140.
Chen, Z., Zhang, Z., Zhai, X., Li, Y., Lin, L., Zhao, H., Bian, L., Li, P., Yu, L., Wu, Y., 2020. Rapid and sensitive detection of anti-SARS-CoV-2 IgG, using lanthanide-doped nanoparticles-based lateral flow immunoassay. Anal. Chem. 92, 7226–7231.
Cho, B., Lee, S.H., Song, J., Bhattacharjee, S., Feng, J., Hong, S., Song, M., Kim, W., Lee, J., Bang, D., 2019a. Nanophotonic cell lysis and polymerase chain reaction with gravity-driven cell enrichment for rapid detection of pathogens. ACS Nano 13, 13866–13874.
Cho, Y.S., Hong, S.C., Choi, J., Jung, J.H., 2019b. Development of an automated wet-cyclone system for rapid, continuous and enriched bioaerosol sampling and its application to real-time detection. Sens. Actuators, B 284, 525–533.
Coker, R.J., Hunter, B.M., Rudge, J.W., Liverani, M., Hanvoravongchai, P., 2011. Emerging infectious diseases in Southeast Asia: regional challenges to control. The Lancet 377, 599–609.
Cooper, J.I., 2012. Viruses and the Environment. Springer Science & Business Media.
Cowling, B.J., Ip, D.K., Fang, V.J., Suntarattiwong, P., Olsen, S.J., Levy, J., Uyeki, T.M., Leung, G.M., Peiris, J.M., Chotpitayasunondh, T., 2013. Aerosol transmission is an important mode of influenza A virus spread. Nat. Commun. 4, 1935.
D'Amore, K., Schulte, A., Kashani, J., 2019. The transmission of the influenza virus from patient to emergency department physician: No flu for you. Am. J. Emergency Med.
De Santis, M., Cavaliere, A.F., Straface, G., Caruso, A., 2006. Rubella infection in pregnancy. Reprod. Toxicol. 21, 390–398.
Devarakonda, S., Singh, R., Bhardwaj, J., Jang, J., 2017. Cost-effective and handmade paper-based immunosensing device for electrochemical detection of influenza virus. Sensors 17, 2597.
Diba, F.S., Kim, S., Lee, H.J., 2015. Amperometric bioaffinity sensing platform for avian influenza virus proteins with aptamer modified gold nanoparticles on carbon chips. Biosens. Bioelectron. 72, 355–361.
Dong, S., Zhao, R., Zhu, J., Lu, X., Li, Y., Qiu, S., Jia, L., Jiao, X., Song, S., Fan, C., Hao, R., Song, H., 2015. Electrochemical DNA biosensor based on a tetrahedral nanostructure probe for the detection of avian influenza A (H7N9) virus. ACS Appl. Mater. Interfaces 7, 8834–8842.
Donkor, E.S., Adegbola, R.A., Wren, B.W., Antonio, M., 2013. Population biology of Streptococcus pneumoniae in West Africa: multilocus sequence typing of serotypes that exhibit different predisposition to invasive disease and carriage. PLoS ONE 8, e53925.
Fang, J., Park, S.-C., Schlag, L., Stauden, T., Pezoldt, J., Jacobs, H.O., 2014. Localized collection of airborne analytes: a transport driven approach to improve the response time of existing gas sensor designs. Adv. Funct. Mater. 24, 3706–3714.
Ferreira, A.P., Werneck, M.M., Ribeiro, R.M., 1999. Aerobiological pathogen detection by evanescent wave fibre optic sensor. Biotechnol. Tech. 13, 447–452.
Fiore, A.E., Shay, D.K., Broder, K., Iskander, J.K., Uyeki, T.M., Mootrey, G., Bresee, J.S., Cox, N.S., 2008. Prevention and control of influenza: recommendations of the Advisory Committee on Immunization Practices (ACIP), 2008. MMWR. Recommendations and reports: Morbidity and mortality weekly report. Recommendations and reports 57, 1–60.
FluView, C., 2011. 2012 influenza season week 45 ending November 12, 2011. Available at. Accessed November 23, 2011.
Fronczek, C.F., Yoon, J.-Y., 2015. Biosensors for monitoring airborne pathogens. J. Lab. Autom. 20, 390–410.
Fu, Y., Romay, V., Liu, Y., Ibarlucea, B., Baraban, L., Khavrus, V., Oswald, S., Bachmatiuk, A., Ibrahim, I., Rümmeli, M., Gemming, T., Bezugly, V., Cuniberti, G., 2017. Chemiresistive biosensors based on carbon nanotubes for label-free detection of DNA sequences derived from avian influenza virus H5N1. Sens. Actuators, B 249, 691–699.
Gandhi, N.R., Nunn, P., Dheda, K., Schaaf, H.S., Zignol, M., Van Soolingen, D., Jensen, P., Bayona, J., 2010. Multidrug-resistant and extensively drug-resistant tuberculosis: a threat to global control of tuberculosis. The Lancet 375, 1830–1843.
Gill, W.P., Harik, N.S., Whiddon, M.R., Liao, R.P., Mittler, J.E., Sherman, D.R., 2009. A replication clock for Mycobacterium tuberculosis. Nat. Med. 15, 211.
Grabowska, I., Malecka, K., Stachyra, A., Góra-Sochacka, A., Sirko, A., Zagórski-Ostoja, W., Radecka, H., Radecki, J., 2013. Single electrode genosensor for simultaneous determination of sequences encoding hemagglutinin and neuraminidase of avian influenza virus type H5N1. Anal. Chem. 85, 10167–10173.
Grisoli, P., Rodolfi, M., Villani, S., Grignani, E., Cottica, D., Berri, A., Picco, A.M., Dacarro, C., 2009. Assessment of airborne microorganism contamination in an industrial area characterized by an open composting facility and a wastewater treatment plant. Environ. Res. 109, 135–142.
Guo, D., Zhuo, M., Zhang, X., Xu, C., Jiang, J., Gao, F., Wan, Q., Li, Q., Wang, T., 2013. Indium-tin-oxide thin film transistor biosensors for label-free detection of avian influenza virus H5N1. Anal. Chim. Acta 773, 83–88.
Hospodsky, D., Yamamoto, N., Peccia, J., 2010. Accuracy, precision, and method detection limits of quantitative PCR for airborne bacteria and fungi. Appl. Environ. Microbiol. 76, 7004–7012.
Hsiao, P.-K., Cheng, C.-C., Chang, K.-C., Yiin, L.-M., Hsieh, C.-J., Tseng, C.-C., 2014. Performance of CHROMagar VRE medium for the detection of airborne vancomycin-resistant/sensitive Enterococcus species. Aerosol Sci. Technol. 48, 173–183.

Huang, C., Wen, T., Shi, F.-J., Zeng, X.-Y., Jiao, Y.-J., 2020. Rapid Detection of IgM Antibodies against the SARS-CoV-2 virus via colloidal gold nanoparticle-based lateral-flow assay. ACS Omega.
Huang, J., Xie, Z., Xie, Z., Luo, S., Xie, L., Huang, L., Fan, Q., Zhang, Y., Wang, S., Zeng, T., 2016. Silver nanoparticles coated graphene electrochemical sensor for the ultrasensitive analysis of avian influenza virus H7. Anal. Chim. Acta 913, 121–127.
Huynh, K.N., Oliver, B.G., Stelzer, S., Rawlinson, W.D., Tovey, E.R., 2008. A new method for sampling and detection of exhaled respiratory virus aerosols. Clin. Infect. Dis. 46, 93–95.
Inami, H., Tsuge, K., Matsuzawa, M., Sasaki, Y., Togashi, S., Komano, A., Seto, Y., 2009. Semi-automated bacterial spore detection system with micro-fluidic chips for aerosol collection, spore treatment and ICAN DNA detection. Biosens. Bioelectron. 24, 3299–3305.
Jarocka, U., Sawicka, R., Góra-Sochacka, A., Sirko, A., Zagórski-Ostoja, W., Radecki, J., Radecka, H., 2014. Electrochemical immunosensor for detection of antibodies against influenza A virus H5N1 in hen serum. Biosens. Bioelectron. 55, 301–306.
Jiang, X., Jing, W., Zheng, L., Liu, S., Wu, W., Sui, G., 2014. A continuous-flow high-throughput microfluidic device for airborne bacteria PCR detection. Lab Chip 14, 671–676.
Jing, W., Jiang, X., Zhao, W., Liu, S., Cheng, X., Sui, G., 2014. Microfluidic platform for direct capture and analysis of airborne Mycobacterium tuberculosis. Anal. Chem. 86, 5815–5821.
Jing, W., Zhao, W., Liu, S., Li, L., Tsai, C.-T., Fan, X., Wu, W., Li, J., Yang, X., Sui, G., 2013. Microfluidic device for efficient airborne bacteria capture and enrichment. Anal. Chem. 85, 5255–5262.
Johnson, H.L., Deloria-Knoll, M., Levine, O.S., Stoszek, S.K., Hance, L.F., Reithinger, R., Muenz, L.R., O'Brien, K.L., 2010. Systematic evaluation of serotypes causing invasive pneumococcal disease among children under five: the pneumococcal global serotype project. PLoS Med. 7, e1000348.
Jonduo, M., Wong, S.-S., Kapo, N., Ominipi, P., Abdad, M., Siba, P., McKenzie, P., Webby, R., Horwood, P., 2013. Surveillance of avian influenza viruses in Papua New Guinean poultry, June 2011 to April 2012. Western Pacific Surveillance Response J.: WPSAR 4, 11.
Jung, J.H., Lee, J.E., Bae, G.-N., 2012. Real-time fluorescence measurement of airborne bacterial particles using an aerosol fluorescence sensor with dual ultraviolet- and visible-fluorescence channels. Environ. Eng. Sci. 29, 987–993.
Källenius, G., Pawlowski, A., Hamasur, B., Svenson, S.B., 2008. Mycobacterial glycoconjugates as vaccine candidates against tuberculosis. Trends Microbiol. 16, 456–462.
Kang, J.S., Lee, K.S., Kim, S.S., Bae, G.-N., Jung, J.H., 2014. Real-time detection of an airborne microorganism using inertial impaction and mini-fluorescent microscopy. Lab Chip 14, 244–251.
Karash, S., Wang, R., Kelso, L., Lu, H., Huang, T.J., Li, Y., 2016. Rapid detection of avian influenza virus H5N1 in chicken tracheal samples using an impedance aptasensor with gold nanoparticles for signal amplification. J. Virol. Methods 236, 147–156.
Karnaushenko, D., Ibarlucea, B., Lee, S., Lin, G., Baraban, L., Pregl, S., Melzer, M., Makarov, D., Weber, W.M., Mikolajick, T., Schmidt, O.G., Cuniberti, G., 2015. Light weight and flexible high-performance diagnostic platform. Adv. Healthcare Mater. 4, 1517–1525.
Kennedy, R., Wakeham, A.J., Byrne, K.G., Meyer, U.M., Dewey, F.M., 2000. A new method to monitor airborne inoculum of the fungal plant pathogens Mycosphaerella brassicicola and Botrytis cinerea. Appl. Environ. Microbiol. 66, 2996–3003.
Kinnamon, D.S., Krishnan, S., Brosler, S., Sun, E., Prasad, S., 2018. Screen printed graphene oxide textile biosensor for applications in inexpensive and wearable point-of-exposure detection of influenza for at-risk populations. J. Electrochem. Soc. 165, B3084–B3090.
Kotwal, G.J., 2008. Genetic diversity-independent neutralization of pandemic viruses (eg HIV), potentially pandemic (eg H5N1 strain of influenza) and carcinogenic (eg HBV and HCV) viruses and possible agents of bioterrorism (variola) by enveloped virus neutralizing compounds (EVNCs). Vaccine 26, 3055–3058.
Kuris, A.M., Lafferty, K.D., Sokolow, S.H., 2014. Sapronosis: a distinctive type of infectious agent. Trends Parasitol. 30, 386–393.
Kwon, H.-J., Fronczek, C.F., Angus, S.V., Nicolini, A.M., Yoon, J.-Y., 2014. Rapid and sensitive detection of H1N1/2009 virus from aerosol samples with a microfluidic immunosensor. J. Lab. Autom. 19, 322–331.
Le, T.T., Adamiak, B., Benton, D.J., Johnson, C.J., Sharma, S., Fenton, R., McCauley, J. W., Iqbal, M., Cass, A.E.G., 2014. Aptamer-based biosensors for the rapid visual detection of flu viruses. Chem. Commun. 50, 15533–15536.
Lednicky, J.A., Loeb, J.C., 2013. Detection and isolation of airborne influenza A H3N2 virus using a sioutas personal cascade impactor sampler. Influenza Res. Treatment 8.
Lee, G.E., Lorch, S.A., Sheffler-Collins, S., Kronman, M.P., Shah, S.S., 2010. National trends in hospitalizations for pediatric community-acquired pneumonia and associated complications. Pediatrics 126, 204.
Lee, J., Ahmed, S.R., Oh, S., Kim, J., Suzuki, T., Parmar, K., Park, S.S., Lee, J., Park, E.Y., 2015. A plasmon-assisted fluoro-immunoassay using gold nanoparticle-decorated carbon nanotubes for monitoring the influenza virus. Biosens. Bioelectron. 64, 311–317.
Lee, J., Jang, J., Akin, D., Savran, C.A., Bashir, R., 2008. Real-time detection of airborne viruses on a mass-sensitive device. Appl. Phys. Lett. 93, 013901.
Lee, J., Morita, M., Takemura, K., Park, E.Y., 2018a. A multi-functional gold/iron-oxide nanoparticle-CNT hybrid nanomaterial as virus DNA sensing platform. Biosens. Bioelectron. 102, 425–431.
Lee, W.S., Kang, T., Kim, S.-H., Jeong, J., 2018b. An antibody-immobilized silica inverse opal nanostructure for label-free optical biosensors. Sensors 18, 307.
Leffel, E.K., Bourdage, J.S., Williamson, E.D., Duchars, M., Fuerst, T.R., Fusco, P.C., 2012. Recombinant protective antigen anthrax vaccine improves survival when administered as a postexposure prophylaxis countermeasure with antibiotic in the New Zealand white rabbit model of inhalation anthrax. Clin. Vaccine Immunol. 19, 1158–1164.
Li, Y., Hong, M., Qiu, B., Lin, Z., Chen, Y., Cai, Z., Chen, G., 2014. Highly sensitive fluorescent immunosensor for detection of influenza virus based on Ag autocatalysis. Biosens. Bioelectron. 54, 358–364.
Li, Z., Yi, Y., Luo, X., Xiong, N., Liu, Y., Li, S., Sun, R., Wang, Y., Hu, B., Chen, W., 2020. Development and clinical application of a rapid IgM-IgG combined antibody test for SARS-CoV-2 infection diagnosis. J. Med. Virol.
Lin, H.-H., Dowdy, D., Dye, C., Murray, M., Cohen, T., 2012. The impact of new tuberculosis diagnostics on transmission: why context matters. Bull. World Health Organ. 90, 739–747.
Liu, Q., Zhang, X., Yao, Y., Jing, W., Liu, S., Sui, G., 2018. A novel microfluidic module for rapid detection of airborne and waterborne pathogens. Sens. Actuators, B 258, 1138–1145.
Liu, X., Cheng, Z., Fan, H., Ai, S., Han, R., 2011. Electrochemical detection of avian influenza virus H5N1 gene sequence using a DNA aptamer immobilized onto a hybrid nanomaterial-modified electrode. Electrochim. Acta 56, 6266–6270.
Liu, Y.-F., Tsai, J.-J., Chin, Y.-T., Liao, E.-C., Wu, C.-C., Wang, G.-J., 2012. Detection of allergies using a silver nanoparticle modified nanostructured biosensor. Sens. Actuators, B 171–172, 1095–1100.
Lynch III, J.P., Zhanel, G.G., 2010. Streptococcus pneumoniae: epidemiology and risk factors, evolution of antimicrobial resistance, and impact of vaccines. Curr. Opin. Pulmonary Med. 16, 217–225.
Magnus, J., Parizel, P.M., Ceulemans, B., Cras, P., Luijks, M., Jorens, P.G., 2011. Streptococcus pneumoniae meningoencephalitis with bilateral basal ganglia necrosis: an unusual complication due to vasculitis. J. Child Neurol. 26, 1438–1443.
Mairhofer, J., Roppert, K., Ertl, P., 2009. Microfluidic systems for pathogen sensing: a review. Sensors 9, 4804–4823.
Marusov, G., Sweatt, A., Pietrosimone, K., Benson, D., Geary, S.J., Silbart, L.K., Challa, S., Lagoy, J., Lawrence, D.A., Lynes, M.A., 2012. A microarray biosensor for multiplexed detection of microbes using grating-coupled surface plasmon resonance imaging. Environ. Sci. Technol. 46, 348–359.
Medina-Sánchez, M., Ibarlucea, B., Pérez, N., Karnaushenko, D.D., Weiz, S.M., Baraban, L., Cuniberti, G., Schmidt, O.G., 2016. High-performance three-dimensional tubular nanomembrane sensor for DNA detection. Nano Lett. 16, 4288–4296.
Millet, J.-P., Moreno, A., Fina, L., Del Baño, L., Orcau, A., De Olalla, P.G., Cayla, J.A., 2013. Factors that influence current tuberculosis epidemiology. Eur. Spine J. 22, 539–548.
Moitra, P., Alafeef, M., Dighe, K., Frieman, M., Pan, D., 2020. Selective naked-eye detection of SARS-CoV-2 mediated by N gene targeted antisense oligonucleotide capped plasmonic nanoparticles. ACS Nano.
Morawska, L., Cao, J., 2020. Airborne transmission of SARS-CoV-2: the world should face the reality. Environ. Int. 105730.
Morens, D.M., Subbarao, K., Taubenberger, J.K., 2012. Engineering H5N1 avian influenza viruses to study human adaptation. Nature 486, 335.
Myatt, T.A., Johnston, S.L., Rudnick, S., Milton, D.K., 2003. Airborne rhinovirus detection and effect of ultraviolet irradiation on detection by a semi-nested RT-PCR assay. BMC Public Health 3, 5.
Nobusawa, E., Sato, K., 2006. Comparison of the mutation rates of human influenza A and B viruses. J. Virol. 80, 3675–3678.
Novel, C., 2010. H1N1 Flu|The 2009 H1N1 Pandemic: Summary Highlights. April 2009–April 2010.
O'Brien, K.L., Wolfson, L.J., Watt, J.P., Henkle, E., Deloria-Knoll, M., McCall, N., Lee, E., Mulholland, K., Levine, O.S., Cherian, T., 2009. Burden of disease caused by Streptococcus pneumoniae in children younger than 5 years: global estimates. The Lancet 374, 893–902.
Organization, W.H., 2013. Rubella reported cases.
Orsini, D.A., Rhoads, K., McElhoney, K., Schick, E., Koehler, D., Hogrefe, O., 2008. A water cyclone to preserve insoluble aerosols in liquid flow—an interface to flow cytometry to detect airborne nucleic acid. Aerosol Sci. Technol. 42, 343–356.
Owen, T.W., Al-Kaysi, R.O., Bardeen, C.J., Cheng, Q., 2007. Microgravimetric immunosensor for direct detection of aerosolized influenza A virus particles. Sens. Actuators, B 126, 691–699.
Pan, Y., Li, X., Yang, G., Fan, J., Tang, Y., Zhao, J., Long, X., Guo, S., Zhao, Z., Liu, Y., 2020. Serological immunochromatographic approach in diagnosis with SARS-CoV-2 infected COVID-19 patients. J. Infect.
Pang, Y., Rong, Z., Wang, J., Xiao, R., Wang, S., 2015. A fluorescent aptasensor for H5N1 influenza virus detection based-on the core–shell nanoparticles metal-enhanced fluorescence (MEF). Biosens. Bioelectron. 66, 527–532.
Pinnick, R.G., Hill, S.C., Nachman, P., Videen, G., Chen, G., Chang, R.K., 1998. Aerosol fluorescence spectrum analyzer for rapid measurement of single micrometer-sized airborne biological particles. Aerosol Sci. Technol. 28, 95–104.
Pyankov, O.V., Agranovski, I.E., Pyankova, O., Mokhonova, E., Mokhonov, V., Safatov, A.S., Khromykh, A.A., 2007. Using a bioaerosol personal sampler in combination with real-time PCR analysis for rapid detection of airborne viruses. Environ. Microbiol. 9, 992–1000.
Rahmani, A.R., Leili, M., Azarian, G., Poormohammadi, A., 2020. Sampling and detection of corona viruses in air: a mini review. Sci. Total Environ. 740, 140207.
Rainer, J., Peintner, U., Pöder, R., 2001. Biodiversity and concentration of airborne fungi in a hospital environment. Mycopathologia 149, 87.
Reef, S.E., Strebel, P., Dabbagh, A., Gacic-Dobo, M., Cochi, S., 2011. Progress toward control of rubella and prevention of congenital rubella syndrome—worldwide, 2009. J. Infect. Dis. 204, S24–S27.

Rota, P.A., Brown, K.E., Hübschen, J.M., Muller, C.P., Icenogle, J., Chen, M.-H., Bankamp, B., Kessler, J.R., Brown, D.W., Bellini, W.J., 2011. Improving global virologic surveillance for measles and rubella. J. Infect. Dis. 204, S506–S513.
Rule, A.M., Schwab, K.J., Kesavan, J., Buckley, T.J., 2009. Assessment of bioaerosol generation and sampling efficiency based on Pantoea agglomerans. Aerosol Sci. Technol. 43, 620–628.
Russell, D.G., Barry, C.E., Flynn, J.L., 2010. Tuberculosis: what we don't know can, and does, hurt us. Science 328, 852–856.
Sakamoto, H., Minpou, Y., Sawai, T., Enami, Y., Suye, S.-I., 2016. A novel optical biosensing system using Mach–Zehnder-type optical waveguide for influenza virus detection. Appl. Biochem. Biotechnol. 178, 687–694.
Sawyer, M.H., Chamberlin, C.J., Wu, Y.N., Aintablian, N., Wallace, M.R., 1994. Detection of varicella-zoster virus DNA in air samples from hospital rooms. J. Infect. Dis. 169, 91–94.
Sengupta, A., Brar, N., Davis, E.J., 2007. Bioaerosol detection and characterization by surface-enhanced Raman spectroscopy. J. Colloid Interface Sci. 309, 36–43.
Sengupta, A., Laucks, M.L., Dildine, N., Drapala, E., Davis, E.J., 2005. Bioaerosol characterization by surface-enhanced Raman spectroscopy (SERS). J. Aerosol Sci. 36, 651–664.
Seo, G., Lee, G., Kim, M.J., Baek, S.-H., Choi, M., Ku, K.B., Lee, C.-S., Jun, S., Park, D., Kim, H.G., 2020. Rapid detection of COVID-19 causative virus (SARS-CoV-2) in human nasopharyngeal swab specimens using field-effect transistor-based biosensor. ACS Nano 14, 5135–5142.
Shen, F., Wang, J., Xu, Z., Wu, Y., Chen, Q., Li, X., Jie, X., Li, L., Yao, M., Guo, X., Zhu, T., 2012. Rapid flu diagnosis using silicon nanowire sensor. Nano Lett. 12, 3722–3730.
Shen, M.-C., Lai, J.-C., Hong, C.-Y., Wang, G.-J., 2017. Electrochemical aptasensor for detecting Der p2 allergen using polycarbonate-based double-generation gold nanoparticle chip. Sens. Bio-Sens. Res. 13, 75–80.
Siegel, J.D., Rhinehart, E., Jackson, M., Chiarello, L., 2007 Guideline for isolation precautions preventing transmission of infectious agents in healthcare settings, 2007.
Singh, R., Hong, S., Jang, J., 2017. Label-free detection of influenza viruses using a reduced graphene oxide-based electrochemical immunosensor integrated with a microfluidic platform. Sci. Rep. 7, 42771.
Skládal, P., Švábenská, E., Žeravík, J., Přibyl, J., Šišková, P., Tjärnhage, T., Gustafson, I., 2012. Electrochemical immunosensor coupled to cyclone air sampler for detection of Escherichia coli DH5α in bioaerosols. Electroanalysis 24, 539–546.
Spencer, R.C., 2003. Bacillus anthracis. J. Clin. Pathol. 56, 182–187.
Stetzenbach, L.D., Buttner, M.P., Cruz, P., 2004. Detection and enumeration of airborne biocontaminants. Curr. Opin. Biotechnol. 15, 170–174.
Sweeney, D.A., Hicks, C.W., Cui, X., Li, Y., Eichacker, P.Q., 2011. Anthrax infection. Am. J. Respir. Crit. Care Med. 184, 1333–1341.
Syedmoradi, L., Ahmadi, A., Norton, M.L., Omidfar, K., 2019. A review on nanomaterial-based field effect transistor technology for biomarker detection. Microchim. Acta 186, 739.
Takemura, K., Adegoke, O., Takahashi, N., Kato, T., Li, T.-C., Kitamoto, N., Tanaka, T., Suzuki, T., Park, E.Y., 2017. Versatility of a localized surface plasmon resonance-based gold nanoparticle-alloyed quantum dot nanobiosensor for immunofluorescence detection of viruses. Biosens. Bioelectron. 89, 998–1005.
Tam, P.D., Van Hieu, N., Chien, N.D., Le, A.-T., Anh Tuan, M., 2009. DNA sensor development based on multi-wall carbon nanotubes for label-free influenza virus (type A) detection. J. Immunol. Methods 350, 118–124.
Tang, J., Li, Y., Eames, I., Chan, P., Ridgway, G., 2006. Factors involved in the aerosol transmission of infection and control of ventilation in healthcare premises. J. Hosp. Infect. 64, 100–114.
Thu, V.V., Tam, P.D., Dung, P.T., 2013. Rapid and label-free detection of H5N1 virus using carbon nanotube network field effect transistor. Curr. Appl Phys. 13, 1311–1315.
Tian, H., Liu, Y., Li, Y., Wu, C.-H., Chen, B., Kraemer, M.U., Li, B., Cai, J., Xu, B., Yang, Q., 2020. An investigation of transmission control measures during the first 50 days of the COVID-19 epidemic in China. Science 368, 638–642.
Tobias, H.J., Schafer, M.P., Pitesky, M., Fergenson, D.P., Horn, J., Frank, M., Gard, E.E., 2005. Bioaerosol mass spectrometry for rapid detection of individual airborne Mycobacterium tuberculosis H37Ra particles. Appl. Environ. Microbiol. 71, 6086–6095.
Tran, T.L., Nguyen, T.T., Huyen Tran, T.T., Chu, V.T., Thinh Tran, Q., Tuan Mai, A., 2017. Detection of influenza A virus using carbon nanotubes field effect transistor based DNA sensor. Physica E 93, 83–86.
Tsai, J.-J., Bau, I.J., Chen, H.-T., Lin, Y.-T., Wang, G.-J., 2011. A novel nanostructured biosensor for the detection of the dust mite antigen Der p2. Int. J. Nanomed. 6, 1201–1208.
Usachev, E.V., Usacheva, O.V., Agranovski, I.E., 2014. Surface plasmon resonance-based bacterial aerosol detection. J. Appl. Microbiol. 117, 1655–1662.
Veerapandian, M., Hunter, R., Neethirajan, S., 2016. Dual immunosensor based on methylene blue-electroadsorbed graphene oxide for rapid detection of the influenza A virus antigen. Talanta 155, 250–257.
Verreault, D., Létourneau, V., Gendron, L., Massé, D., Gagnon, C.A., Duchaine, C., 2010. Airborne porcine circovirus in Canadian swine confinement buildings. Vet. Microbiol. 141, 224–230.
Wakeham, A., Kennedy, R., McCartney, A., 2004. The collection and retention of a range of common airborne spore types trapped directly into microtiter wells for enzyme-linked immunosorbent analysis. J. Aerosol Sci. 35, 835–850.
Wang, Z.-Z., Zheng, Z., Wang, X.-C., Zheng, P.-M., Cui, F.-C., Zhou, Q.-W., Hu, H.-Z., Li, X.-Q., Zhang, H.-L., Wei, Y.-X., 2020. Rapid Detection of Anti-SARS-CoV-2 IgM and IgG Using a Selenium Nanoparticle-based Lateral Flow Immunoassay.
Weber, T.P., Stilianakis, N.I., 2008. Inactivation of influenza A viruses in the environment and modes of transmission: a critical review. J. Infect. 57, 361–373.
Wen, T., Huang, C., Shi, F.-J., Zeng, X.-Y., Lu, T., Ding, S.-N., Jiao, Y.-J., 2020. Development of a lateral flow immunoassay strip for rapid detection of IgG antibody against SARS-CoV-2 virus. Analyst.
West, J.S., Kimber, R.B.E., 2015. Innovations in air sampling to detect plant pathogens. Ann. Appl. Biol. 166, 4–17.
WHO, WH, O., 2012. Global Tuberculosis Report. World Health Organization.
Wilson, G.A., DeFreez, R.K., 2004. Multispectral-diode-laser-induced fluorescence biological particle sensor. SPIE.
Wu, Z., Guo, W.-J., Bai, Y.-Y., Zhang, L., Hu, J., Pang, D.-W., Zhang, Z.-L., 2018. Digital single virus electrochemical enzyme-linked immunoassay for ultrasensitive H7N9 avian influenza virus counting. Anal. Chem. 90, 1683–1690.
Xu, L., Wang, R., Kelso, L.C., Ying, Y., Li, Y., 2016. A target-responsive and size-dependent hydrogel aptasensor embedded with QD fluorescent reporters for rapid detection of avian influenza virus H5N1. Sens. Actuators, B 234, 98–108.
Zhan, L., Li, C.M., Wu, W.B., Huang, C.Z., 2014. A colorimetric immunoassay for respiratory syncytial virus detection based on gold nanoparticles–graphene oxide hybrids with mercury-enhanced peroxidase-like activity. Chem. Commun. 50, 11526–11528.
Zhan, L., Zhen, S.J., Wan, X.Y., Gao, P.F., Huang, C.Z., 2016. A sensitive surface-enhanced Raman scattering enzyme-catalyzed immunoassay of respiratory syncytial virus. Talanta 148, 308–312.
Zhou, C.-H., Zhao, J.-Y., Pang, D.-W., Zhang, Z.-L., 2014. Enzyme-induced metallization as a signal amplification strategy for highly sensitive colorimetric detection of avian influenza virus particles. Anal. Chem. 86, 2752–2759.
Zhu, X., Ai, S., Chen, Q., Yin, H., Xu, J., 2009. Label-free electrochemical detection of Avian Influenza Virus genotype utilizing multi-walled carbon nanotubes–cobalt phthalocyanine–PAMAM nanocomposite modified glassy carbon electrode. Electrochem. Commun. 11, 1543–1546.